Analysis of characteristic differentiation processes at the single cell level

JI-HYE CHUNG

2016

Contents

Abbreviations

ANOVA	Analysis of variance
CID	Collision-induced dissociation
CRISPR	Clustered regularly interspaced short palindromic repeats
DAVID	Database for annotation, visualization and integrated discovery
DMEM	Dulbecco's modified Eagle's medium
DMSO	Dimethyl sulfoxide
EPLIN	Epithelial protein lost in neoplasm
ERK	Extracellular signal-regulated kinase
ESI	Electrospray ionization
FACS	Fluorescence-activated cell sorting
FBS	Fetal bovine serum
GAPDH	Glyceraldehyde-3-phosphate dehydrogenase
GFP	Green fluorescent protein
GO	Gene ontology
HEK	Human embryonic kidney
HRP	Horse radish peroxidase
IgG	Immunoglobulin G
IQR	Inter quartile range
LC	Liquid chromatography
LHR	Left homologous region
MDCK	Madin-Darby canine kidney
MEK	Mitogen-activated protein kinase kinase
MS	Mass spectrometry
NGF	Nerve growth factor
PAGE	Polyacrylamide gel electrophoresis
PBS	Phosphate buffered saline
PCR	Polymerase chain reaction
RHR	Right homologous region
SDS	Sodium dodecyl sulfate

TEAB	Triethyl ammonium bicarbonate
TrkA	Tropomyosin receptor kinase A

Introduction

Among the various biological processes that are necessary for maintaining life of a multicellular organism, cell differentiation is involved in stages from as early as embryonic development to the later stages of life. Maintaining a balance between proliferation and differentiation in stem cells is known to be the key factor for controlling homeostasis of various organs including the epidermis (1), intestines (2, 3), and brain (4). Dysregulation of this balance leads to pathological conditions such as obesity resulting from facilitated adipocyte differentiation (5) and type 2 diabetes resulting from beta-cell dedifferentiation (6). In particular, disordered control of the cell differentiation state is known to be deeply related to the aggressiveness of cancer, which is one of the leading causes of death worldwide (7, 8).

Until recently, experimental methods used for the research of biological processes, such as cell differentiation, mainly involved obtaining information from thousands of cells in total. When these conventional approaches of bulk analysis are applied to analyze a group of cells, the information from individual cells in the group is averaged, resulting in the masking of rare but important traits of each single cell. However, studies based on single-cell analyses have revealed that even cells that are cultured and treated under the same conditions have distinct characteristics from one another. In particular, such heterogeneity among cells has been shown to affect diverse levels of differentiation that proceeds along time (9-11). Therefore, to precisely understand a heterogeneous process such as cell differentiation, it is necessary to capture and analyze characteristics of single cells and changes that occur over time.

Cell differentiation process

Cell differentiation is a process in which less specialized pluripotent stem cells change into various mature cell types that are functionally more specialized. Pluripotent stem cells are characterized by their ability to both self-replicate through cell division and give rise to new types of cells that have more specialized biological features (Fig. 1). The experimental method to derive embryonic stem cells from early mouse embryos was discovered in 1981 (12, 13), and this discovery made it possible to manipulate and analyze the differentiation process *in vitro*. When these cells receive differentiation-inducing signals from stimulants such as growth factors,

hormones, small molecules, pH, or temperature, progressive changes occur in the genetic expression profiles, cell morphology, and physiological functions.

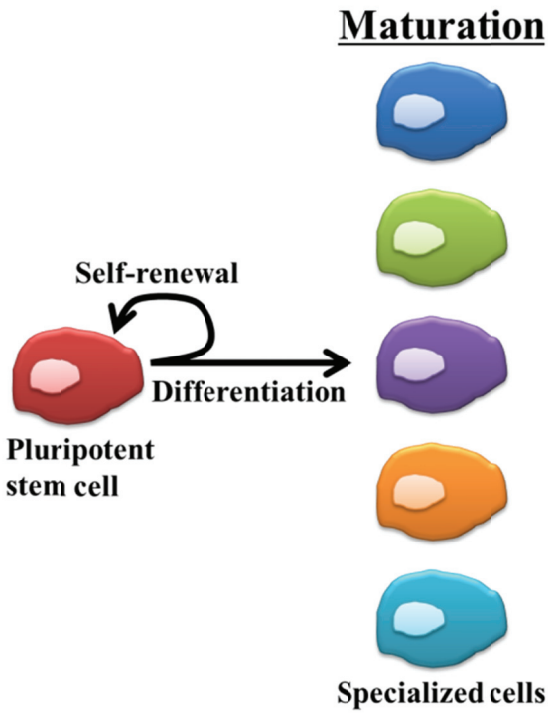

Fig. 1 Cell differentiation process

As a result of thorough investigation of differentiation-inducing cues and their molecular mechanisms, methods to direct stem cells into certain specialized cell types *in vitro* have been developed. It has been reported that embryonic stem cells can be directed to differentiate into various cell types such as neurons (14), chondrocytes (15), or thymic epithelial cells (16) by treatment with growth factors and chemicals that alter signaling pathways inside the target cells. These *in vitro* models of cell differentiation are considered to be important tools not only for the study of the embryonic development process but also for the research of numerous diseases and practical application for therapies such as cell transplantation (14-16).

Model for neuronal cell differentiation

Among the wide variety of *in vitro* models for cell differentiation processes, the PC12 cell line, which is derived from a pheochromocytoma of the rat adrenal medulla (17), is one of the most well-recognized cell lines utilized for the study of the neuronal differentiation process and diseases (18, 19). PC12 cells are a useful model because of their capacity to differentiate into neuron-like cells with neurite-like projections when exposed to nerve growth factor (NGF) [Fig. 2(a)]. When NGF is added to the culture medium of PC12, it binds to tropomyosin receptor kinase A (TrkA), which is a cell-surface receptor that has phosphorylation activity leading to the activation of the mitogen-activated protein kinase kinase (MEK)/extracellular signal-regulated kinase (ERK) signaling pathway [Fig. 2(b)]. As a result of this activation of the MEK/ERK signaling pathway, PC12 cells differentiate into neuron-like cells (20).

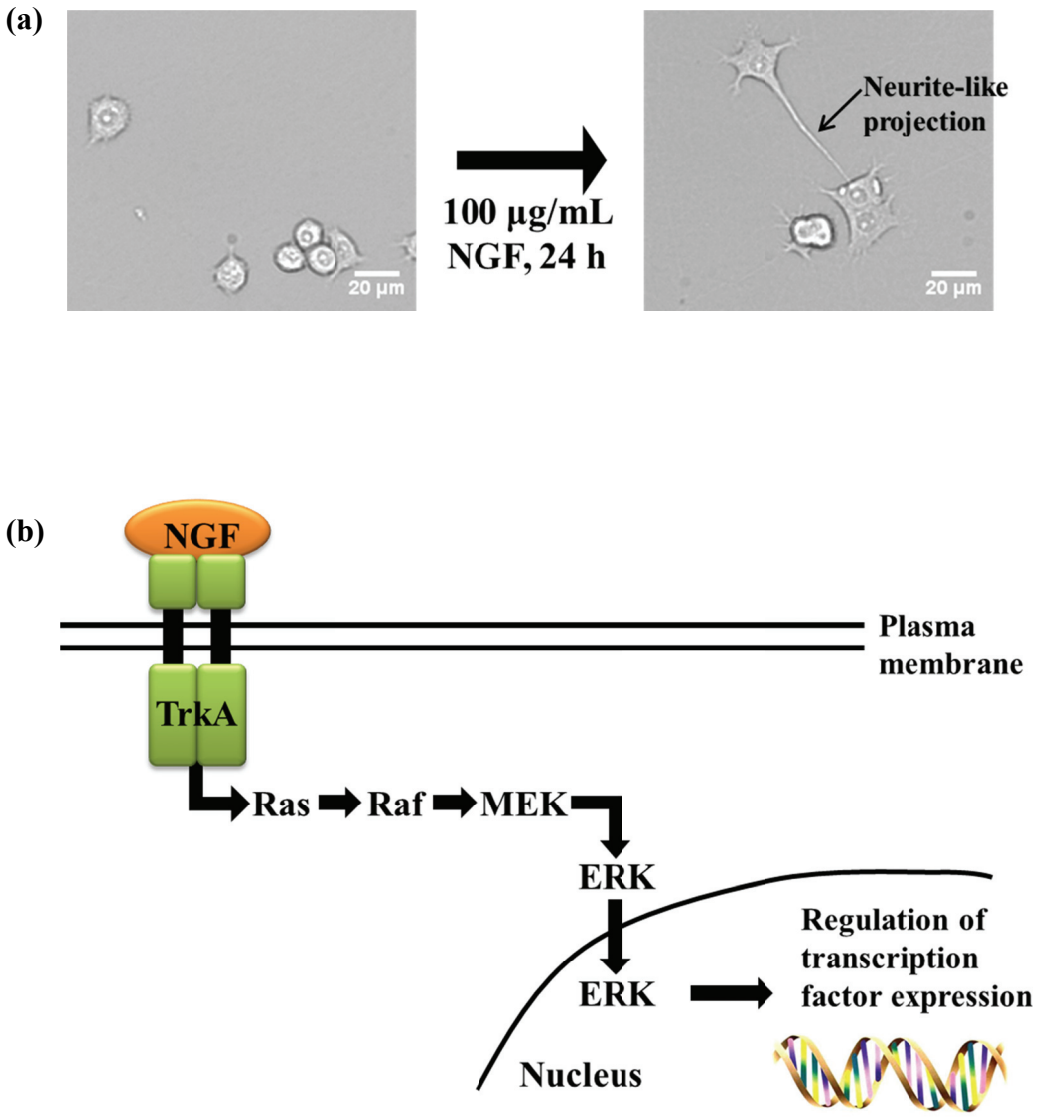

Fig. 2 Neuronal differentiation of PC12 cells induced by NGF (a). MEK/ERK signaling pathway underlying the differentiation process of PC12 cells (b).

NGF: nerve growth factor, TrkA: tropomyosin receptor kinase A, MEK: mitogen-activated protein kinase kinase, ERK: extracellular signal-regulated kinase

Previous studies have indicated that small-molecule inhibitors of the MEK/ERK pathway components can suppress neuronal differentiation in PC12 cells, resulting in reduction of the outgrowth of neurites (21, 22). However, simply adding the substances to the medium does not enable precise quantification of the amount of molecules that are actually introduced into individual target cells. Moreover, conventional methods of bulk analysis of thousands of cells as a group have not been capable of providing sufficient quantified information on phenotypic changes occurring in single target cells during the differentiation process. To obtain a clearer view of the modifications that each single cell undergoes during the neuronal differentiation process and the effects of small-molecule substances on each target single cell, it is necessary to conduct quantifiable analyses that are more closely focused on each single cell.

Cellular competition induced by cancer-related gene transformation

Cancer is one of the most well-known diseases that involve dysregulation of the cell differentiation state. As cancer progresses, cells lose the expression of tissue or organ-specific marker genes and undergo unregulated cell division. Clinical studies have also revealed that the differentiation state of cancer cells is related to the metastatic ability and prognosis of cancer (7, 8).

Molecular biological research on various types of cancers has led to the identification of numerous oncogenes and tumor suppressor genes that are involved in the cancer development process (Table 1). Many of these genes are known to be involved in cellular procedures such as cell cycle control, DNA repair, apoptosis, etc. These identified genes have been utilized in cancer therapy as targets for drug development or markers for diagnosis. Research for cancer control has mainly focused on the genetic transformations in cancer cells themselves and the changes that occur in the cells when they obtain certain cancer-related transformations.

Table 1 Cancer-related genes (23)

Gene categories	Genes	Related cancer
Oncogenes	*HER2*	Breast cancer, Lung cancer
	EGFR	Lung cancer, Colon cancer
	BCR-ABL	Leukemia
	B-RAF	Skin cancer
	BCL-3	Lymphoma
Tumor suppressors	*RB1*	Retinoblastoma
	HNPCC	Colon cancer, Endometrial cancer
	P53	Lung cancer, Colon cancer, Breast cancer, Brain cancer

However, the fact that cancer cells are surrounded by normal cells in an organism has not been the main emphasis of cancer research. In the very early stages of cancer development, cancer-related gene transformation occurs in a single cell and the disease progresses as the cell grows and obtains additional gene transformations. Cells that bear these gene transformations are present in a microenvironment in which they must compete with surrounding normal cells, which exist in much larger numbers. Recently, several studies using *Drosophila melanogaster* or mammalian cell cultures showed that when cells with cancer-related gene transformation are co-cultured with normal cells, an interaction occurs between the two types of cells, resulting in elimination from the cell layer or apoptosis of one of the cell types that has been outcompeted by the other (Fig. 3) (24-26). By concentrating on this interaction between cancer-related transformed and surrounding normal cells, a completely new apporach toward cancer control, such as exploiting surrounding cells to attack newly arising cancer cells, can become possible.

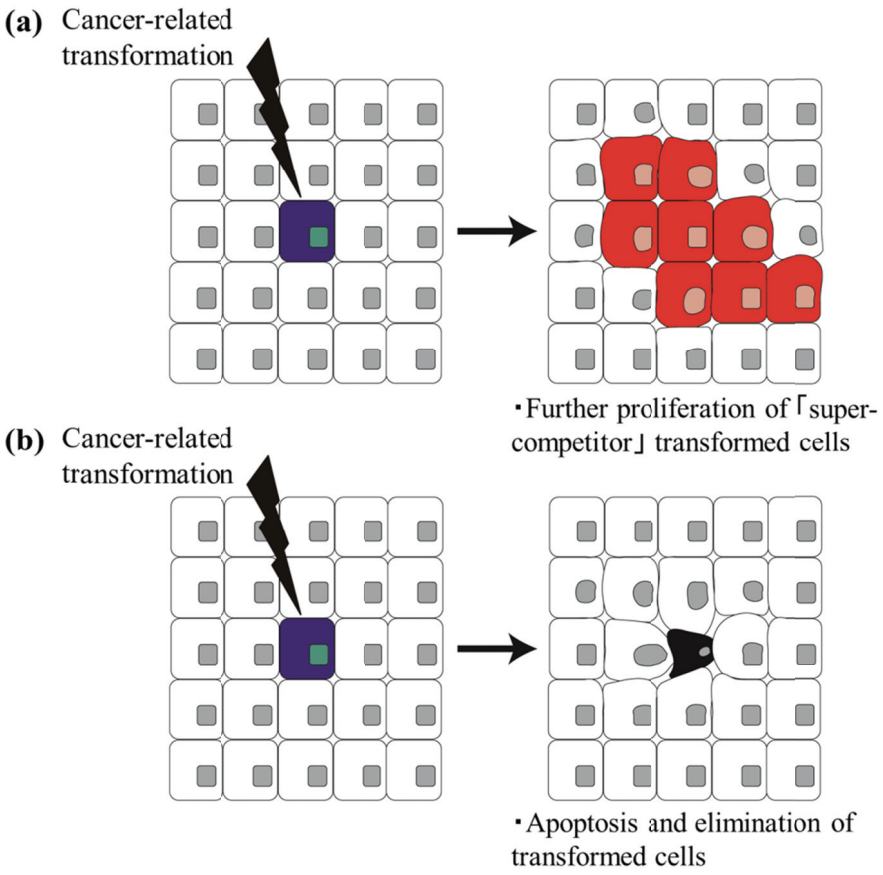

Fig. 3 Two types of intercellular interaction in *in vitro* model of cancer development

Proliferation of the 「super-competitor」 transformed cells when co-cultured with the wild-type cells (a). Elimination of the transformed cells outcompeted by the surrounding wild-type cells (b).

To understand the underlying processes and to effectively take advantage of the molecules that play critical roles, the molecular mechanism of mutual recognition and interaction between the transformed and normal cells must be elucidated in detail.

Conventional methods for the research of biological processes

In conventional experimental methods that have long been used for a wide range of biological studies, the target for various analyses has been groups of cells comprising thousands of cells. Generally, the existing methods involve cellular alterations achieved by introducing exogenous genetic materials or adding cell-permeable substances to the culture medium (27-30). However, when exogenous genes are introduced into the cells using viral vectors or plasmids, it is impossible to precisely measure and control the amount of proteins in each target cell, which are the actual functioning molecules produced as a result of gene expression (Fig. 4). In addition, when cell-permeable substances are introduced into the target cells by simply adding them to the culture medium, it is impossible to accurately regulate the amount of molecules that actually enter into each single cell and function (Fig. 4).

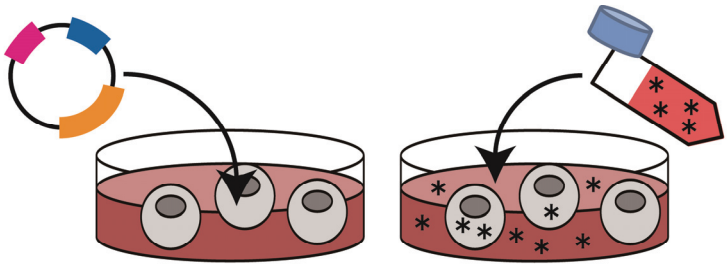

Impossible to measure actual amount of functioning molecules

Fig. 4 Problem with conventional methods for cellular alteration

Moreover, molecular and physiological changes of the target cells that occur as a result of cellular alteration have been analyzed by measuring the averaged composition of biomolecules including proteins, metabolites, and genes in thousands of cells by bulk analysis. These methods are performed under the assumption that the averaged information obtained from all cells as a total reflects the identical characteristics of all target cells. However, recent improvements in experimental techniques for single-cell analysis have indicated that these averaged measurements of bulk analysis do not reflect the heterogeneous nature of cell populations. As a result of combining various advanced experimental approaches, such as high-resolution imaging, single-cell omics analysis, flow cytometry, and microfluidics, it has been discovered that regulation of gene expression and protein production is highly heterogeneous even in individual single cells that are treated under the same condition (31-33). In particular, cell differentiation has been shown to be a stochastic process which occurs in a heterogeneous manner, with the existence of distinct cell types of a variety of differentiation states (Fig. 5) (9-11).

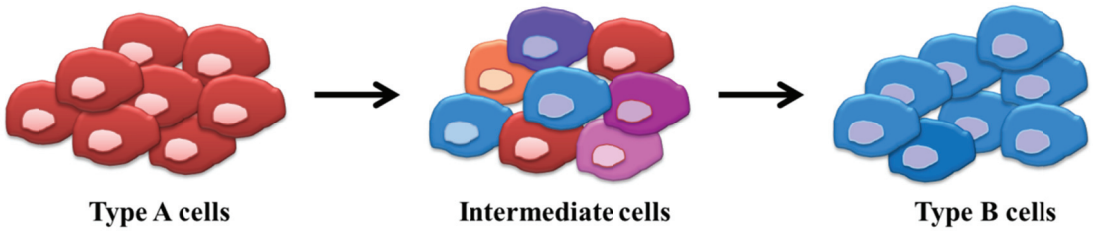

Fig. 5 Heterogeneous nature of the cell differentiation process

This fact has been hindering the obtainment of accurate information about individual cells going through various differentiation processes and the application of the collected data for practical purposes such as disease research or drug development. To solve the problems of conventional experimental methods based on bulk analysis, it is essential to focus on the techniques of single-cell analysis by which each target cell can be manipulated and analyzed in an accurate and quantifiable manner.

References

1. **Pankow S, Bamberger C, Klippel A, Werner S.** 2006. Regulation of epidermal homeostasis and repair by phosphoinositide 3-kinase. J Cell Sci **119:**4033-4046.
2. **Barker N, van Es JH, Kuipers J, Kujala P, van den Born M, Cozijnsen M, Haegebarth A, Korving J, Begthel H, Peters PJ, Clevers H.** 2007. Identification of stem cells in small intestine and colon by marker gene Lgr5. Nature **449:**1003-1007.
3. **Dow LE, O'Rourke KP, Simon J, Tschaharganeh DF, van Es JH, Clevers H, Lowe SW.** 2015. Apc restoration promotes cellular differentiation and reestablishes crypt homeostasis in colorectal cancer. Cell **161:**1539-1552.
4. **Johansson CB, Svensson M, Wallstedt L, Janson AM, Frisen J.** 1999. Neural stem cells in the adult human brain. Exp Cell Res **253:**733-736.
5. **Lee H, Lee YJ, Choi H, Ko EH, Kim JW.** 2009. Reactive oxygen species facilitate adipocyte differentiation by accelerating mitotic clonal expansion. J Biol Chem **284:**10601-10609.
6. **Dor Y, Glaser B.** 2013. Beta-cell dedifferentiation and type 2 diabetes. N Engl J Med **368:**572-573.
7. **Sommers CL, Byers SW, Thompson EW, Torri JA, Gelmann EP.** 1994. Differentiation state and invasiveness of human breast cancer cell lines. Breast Cancer Res Treat **31:**325-335.
8. **Jogi A, Vaapil M, Johansson M, Pahlman S.** 2012. Cancer cell differentiation heterogeneity and aggressive behavior in solid tumors. Ups J Med Sci **117:**217-224.
9. **Smith ZD, Nachman I, Regev A, Meissner A.** 2010. Dynamic single-cell imaging of direct reprogramming reveals an early specifying event. Nat Biotechnol **28:**521-526.
10. **Narsinh KH, Sun N, Sanchez-Freire V, Lee AS, Almeida P, Hu S, Jan T, Wilson KD,**

Leong D, Rosenberg J, Yao M, Robbins RC, Wu JC. 2011. Single cell transcriptional profiling reveals heterogeneity of human induced pluripotent stem cells. J Clin Invest **121:**1217-1221.

11. **Gerlach C, Rohr JC, Perie L, van Rooij N, van Heijst JW, Velds A, Urbanus J, Naik SH, Jacobs H, Beltman JB, de Boer RJ, Schumacher TN.** 2013. Heterogeneous differentiation patterns of individual CD8+ T cells. Science **340:**635-639.
12. **Martin GR.** 1981. Isolation of a pluripotent cell line from early mouse embryos cultured in medium conditioned by teratocarcinoma stem cells. Proc Natl Acad Sci USA **78:**7634-7638.
13. **Evans MJ, Kaufman MH.** 1981. Establishment in culture of pluripotential cells from mouse embryos. Nature **292:**154-156.
14. **Wichterle H, Lieberam I, Porter JA, Jessell TM.** 2002. Directed differentiation of embryonic stem cells into motor neurons. Cell **110:**385-397.
15. **Oldershaw RA, Baxter MA, Lowe ET, Bates N, Grady LM, Soncin F, Brison DR, Hardingham TE, Kimber SJ.** 2010. Directed differentiation of human embryonic stem cells toward chondrocytes. Nat Biotechnol **28:**1187-1194.
16. **Sun X, Xu J, Lu H, Liu W, Miao Z, Sui X, Liu H, Su L, Du W, He Q, Chen F, Shi Y, Deng H.** 2013. Directed differentiation of human embryonic stem cells into thymic epithelial progenitor-like cells reconstitutes the thymic microenvironment *in vivo*. Cell Stem Cell **13:**230-236.
17. **Greene LA, Tischler AS.** 1976. Establishment of a noradrenergic clonal line of rat adrenal pheochromocytoma cells which respond to nerve growth factor. Proc Natl Acad Sci USA **73:**2424-2428.
18. **Fox JH, Barber DS, Singh B, Zucker B, Swindell MK, Norflus F, Buzescu R,**

Chopra R, Ferrante RJ, Kazantsev A, Hersch SM. 2004. Cystamine increases L-cysteine levels in Huntington's disease transgenic mouse brain and in a PC12 model of polyglutamine aggregation. J Neurochem **91:**413-422.

19. **Johnson G, Refolo LM, Wallace W.** 1993. Heat-shocked neuronal PC12 cells reveal Alzheimer's disease-associated alterations in amyloid precursor protein and tau. Ann N Y Acad Sci **695:**194-197.

20. **Vaudry D, Stork PJ, Lazarovici P, Eiden LE.** 2002. Signaling pathways for PC12 cell differentiation: making the right connections. Science **296:**1648-1649.

21. **Favata MF, Horiuchi KY, Manos EJ, Daulerio AJ, Stradley DA, Feeser WS, Van Dyk DE, Pitts WJ, Earl RA, Hobbs F, Copeland RA, Magolda RL, Scherle PA, Trzaskos JM.** 1998. Identification of a novel inhibitor of mitogen-activated protein kinase kinase. J Biol Chem **273:**18623-18632.

22. **Das KP, Freudenrich TM, Mundy WR.** 2004. Assessment of PC12 cell differentiation and neurite growth: a comparison of morphological and neurochemical measures. Neurotoxicol Teratol **26:**397-406.

23. **Collins FS, Barker AD.** 2007. Mapping the cancer genome. Pinpointing the genes involved in cancer will help chart a new course across the complex landscape of human malignancies. Sci Am **296:**50-57.

24. **Moreno E, Basler K.** 2004. dMyc transforms cells into super-competitors. Cell **117:**117-129.

25. **Tamori Y, Bialucha CU, Tian AG, Kajita M, Huang YC, Norman M, Harrison N, Poulton J, Ivanovitch K, Disch L, Liu T, Deng WM, Fujita Y.** 2010. Involvement of Lgl and Mahjong/VprBP in cell competition. PLoS Biol **8:**e1000422.

26. **Norman M, Wisniewska KA, Lawrenson K, Garcia-Miranda P, Tada M, Kajita M,**

Mano H, Ishikawa S, Ikegawa M, Shimada T, Fujita Y. 2012. Loss of Scribble causes cell competition in mammalian cells. J Cell Sci **125:**59-66.

27. **Huangfu D, Maehr R, Guo W, Eijkelenboom A, Snitow M, Chen AE, Melton DA.** 2008. Induction of pluripotent stem cells by defined factors is greatly improved by small-molecule compounds. Nat Biotechnol **26:**795-797.

28. **Okita K, Nakagawa M, Hyenjong H, Ichisaka T, Yamanaka S.** 2008. Generation of mouse induced pluripotent stem cells without viral vectors. Science **322:**949-953.

29. **Zhou H, Wu S, Joo JY, Zhu S, Han DW, Lin T, Trauger S, Bien G, Yao S, Zhu Y, Siuzdak G, Scholer HR, Duan L, Ding S.** 2009. Generation of induced pluripotent stem cells using recombinant proteins. Cell Stem Cell **4:**381-384.

30. **Ieda M, Fu JD, Delgado-Olguin P, Vedantham V, Hayashi Y, Bruneau BG, Srivastava D.** 2010. Direct reprogramming of fibroblasts into functional cardiomyocytes by defined factors. Cell **142:**375-386.

31. **Weinberger LS, Burnett JC, Toettcher JE, Arkin AP, Schaffer DV.** 2005. Stochastic gene expression in a lentiviral positive-feedback loop: HIV-1 Tat fluctuations drive phenotypic diversity. Cell **122:**169-182.

32. **Toriello NM, Douglas ES, Thaitrong N, Hsiao SC, Francis MB, Bertozzi CR, Mathies RA.** 2008. Integrated microfluidic bioprocessor for single-cell gene expression analysis. Proc Natl Acad Sci USA **105:**20173-20178.

33. **Wang D, Bodovitz S.** 2010. Single cell analysis: the new frontier in 'omics'. Trends Biotechnol **28:**281-290.

Chapter I Single-cell analysis of PC12 neuronal differentiation process using direct microinjection method

Cell differentiation is an important target for biological research, because it is a critical process for development of multicellular organisms and maintenance of homeostasis in various organs such as the epidermis (1), intestines (2, 3), and brain (4). Types of cells with specialized functions arise from pluripotent stem cells through cell differentiation process, and dysregulation of this process may lead to pathological conditions such as obesity resulting from facilitated adipocyte differentiation (5) and type 2 diabetes resulting from beta-cell dedifferentiation (6).

Until recently, experimental methods used for the research of various cell differentiation processes mainly involved obtaining information from thousands of cells in total. In these methods of bulk analysis of a group of cells, it is considered that the averaged results reflect the identical characteristics of all cells in the target group. Generally, existing methods for cellular alteration based on this concept involve introduction of exogenous genetic materials by transfection or addition of cell-permeable substances in culture medium (7-10). These methods make it difficult to precisely measure and control the amount of regulation factors that are actually introduced into each target cell. However, recent studies based on single-cell analysis have indicated the genomic and phenotypic differences among individual cells in the same population cultured and treated under identical conditions (11-13). Particularly, advanced techniques for isolation and analysis of single cells have revealed that such heterogeneity among cells effects diverse levels of differentiation in somatic cells or induced pluripotent stem cells (14-16). This heterogeneity among individual cells leads to the obscuration of minor but critical changes that each cell undergoes during cell differentiation, hindering safe and efficient application of novel techniques for regulating mammalian cell differentiation (14, 17).

Among the wide variety of *in vitro* models for cell differentiation processes, the PC12 cell line, which is derived from a pheochromocytoma of the rat adrenal medulla (18), is one of the most well-recognized cell lines utilized for the study of the neuronal differentiation process and diseases (19, 20). PC12 cells are a useful model for study on neuronal differentiation or diseases (19, 21), because of their characteristic to differentiate into neuron-like cells when

exposed to nerve growth factor (NGF) (18). Neuronal differentiation of PC12 can be inhibited by adding U0126, an inhibitor of mitogen-activated protein kinase kinase (MEK), to the culture medium (22); however, simply adding the chemical to the cell culture medium does not enable precise quantification of the amount of U0126 molecules that are actually introduced into individual cells. In addition, bulk analysis of the cells makes it difficult to keep track of phenotypic changes occurring on each target cell during the differentiation process.

To solve these problems of conventional experimental procedures, we attempted to inhibit the NGF-induced differentiation of PC12 cells quantitatively by directly introducing U0126 molecules into individual target cells using the automated microinjection system. Moreover, time-course phenotypic changes that occur on each target PC12 cell was analyzed at the single cell level, as an attempt to clarify the heterogeneous nature of cell differentiation process.

Materials and Methods

Preparation of surface-coated culture dishes for cultivation of PC12 cells

Substrates for coating the surface of culture dishes (laminin, collagen, poly-L-lysine, and gelatin) were prepared as solutions of the indicated concentrations in 1× phosphate buffered saline (PBS, 137 mM NaCl, 8.1 mM Na_2HPO_4, 2.68 mM KCl, 1.47 mM KH_2PO_4, pH7.4, NIPPON GENE, Japan). Each solution was added onto 35 mm non-coated cell culture dish (BD Falcon, USA), and the dishes were incubated at room temperature for six hours. Then the substrate solution was removed and the dishes were washed with 1 mL of PBS before seeding the PC12 cells.

Preparation of 35 mm dishes for induction and inhibition of PC12 differentiation

PC12 cells (No. CRL-1721, ATCC, USA) were cultured in Dulbecco's modified Eagle's medium (DMEM, Nacalai Tesque, Japan) supplemented with 10% (v/v) fetal bovine serum (FBS) and 5% (v/v) heat-inactivated horse serum (all from Gibco, USA). Cells that were fluorescently stained with Celltracker™ Green (Lonza, Switzerland) and cells with no stain were mixed at a ratio of 1:2. Mixed cells were seeded on laminin-coated 35 mm dishes at 1.2 ×

10^5 cells per dish. In experiments using the cell culture medium containing U0126, 6.0×10^5 unstained cells were seeded on each 35 mm dish. All dishes were incubated at 37°C in humidified atmosphere with 95% air and 5% CO_2.

Automated microinjection

Throughout experiments, injection of various solutions into the target PC12 cells was performed using the automated microinjection device developed by Fujitsu Ltd. (CI-2500, http://www.fujitsu.com). Injections were performed using a glass capillary with an inner diameter of 0.5 μm and an outer diameter of 1.0 μm (Femtotips I, Eppendorf, Germany). Steps such as positioning of the dish and capillary, and adjusting the microscopic focus on the capillary and the target cells, were automated by using CI-2500 (23).

For validation of injection volume control by CI-2500, Texas Red (dextran conjugated, MW 10 kD, Invitrogen, USA) was dissolved in 1× PBS (pH7.4) to 1 mg/mL. Injection of the fluorescence solution was repeated 32 times for each indicated volume, and images before and after each injection were obtained using the microscope attached to the microinjector. The fluorescence filter set with a 560 ± 30 nm excitation filter, a 645 ± 40 nm emission filter, and a 595 nm dichroic mirror (XF102-2, Omega Optical, USA) was used for the detection of Texas Red fluorescence. Fluorescence intensities were analyzed by measuring the difference in total gray value of images obtained before and after each injection, using the NIH ImageJ software (http://rsbweb.nih.gov/ij/).

Direct injection of U0126 into PC12 cells

To confirm that there was no physical effect of microinjection on PC12 differentiation, neurite length on cells injected only with the fluorescence marker solution (1 mg/mL Texas Red in 1× PBS) was compared with control cells without injection. In each target cell, 0.25 pL was injected, and PC12 differentiation was induced by adding 2.5S NGF (Invitrogen, USA) to the culture medium at 100 ng/mL. Neurite outgrowth was analyzed by manually tracing and measuring neurite lengths in cell images after 48 h using ImageJ software.

U0126 (Wako, Japan)/dimethyl sulfoxide (DMSO) solution was diluted to different concentrations using PBS, and mixed with 1 mg/mL Texas Red. Only Celltracker^{TM}-stained cells in the mix-culture dishes were selected as the targets for injection and further analysis (Fig.

1). Induction of PC12 neuronal differentiation and measurement of neurite length in differentiated cells were done as described above. For the detection of Celltracker^{TM} Green fluorescence, the fluorescence filter set with a 460–495 nm excitation filter, a 510 IF emission filter, and a 505 nm dichroic mirror (U-MWIB3, Olympus, Japan) was used.

Addition of U0126 to culture medium of PC12

U0126/DMSO solution was added to culture medium at the indicated concentrations along with NGF. Total number of molecules added to each dish was calculated using Avogadro's constant (N_A=6.02 × 10^{23} mol^{-1}), and the volume of culture medium on each dish (V=1.2 mL), and the number was divided by total number of cells growing on each dish (6.0 × 10^5 cells).

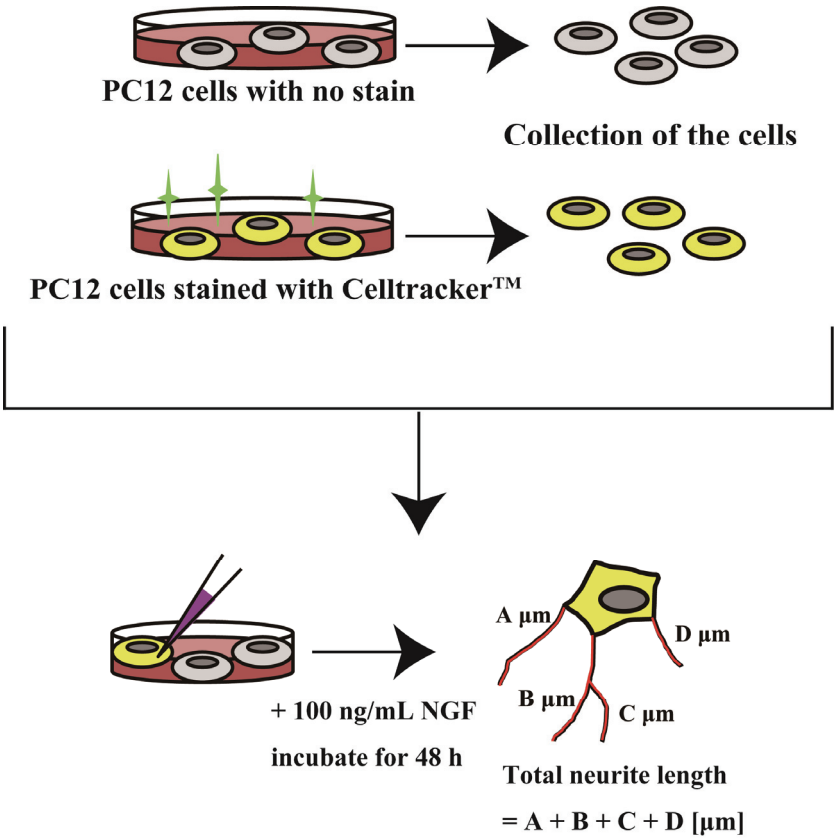

Fig. 1 Schematic diagram of the experimental procedure of U0126 injection

Statistical analysis

Non-parametric Mann-Whitney *U* test was used to examine the significance of differences in neurite outgrowth between cells injected with Texas Red solution and the control. For the U0126 injection experiments, results of neurite length analyses were compiled from three individual experiments that were performed under the same conditions. Data sets obtained from each experiment were confirmed to show no significant differences from each other using the Kruskal-Wallis test under all injection volumes. The non-parametric Kruskal-Wallis test followed by Shirley-Williams test was used for pairwise statistical comparison of neurite length in cells injected with U0126 and control group of cells injected with the solvent only (24). For the experiments using culture medium containing U0126, single-factor analysis of variance (ANOVA) was performed in order to confirm the significance of the inhibitive effect. A statistically significant difference is indicated by $*P < 0.05$ and $**P < 0.01$.

Results

Applicability of microinjection method to inhibition of PC12 differentiation

To achieve the highest efficiency of introducing the differentiation inhibitor into the target cells, optimization of the experimental conditions and confirmation of the applicability of the method was performed. When the differentiation inhibitor solution is injected into the target cells that are cultivated on the surface of a plastic dish, physical contact between the glass capillary of the microinjector and the target cell occurs. To minimize the influence of this contact on the target cells, surface-coating substrate was optimized to achieve the strongest attachment of the cells on the dish surface and maintenance of the single-cell state of the cultured cells. The results showed that laminin was the most appropriate substrate for the coating of the dishes to cultivate the target PC12 cells and perform direct microinjection to the cells (Fig. 2).

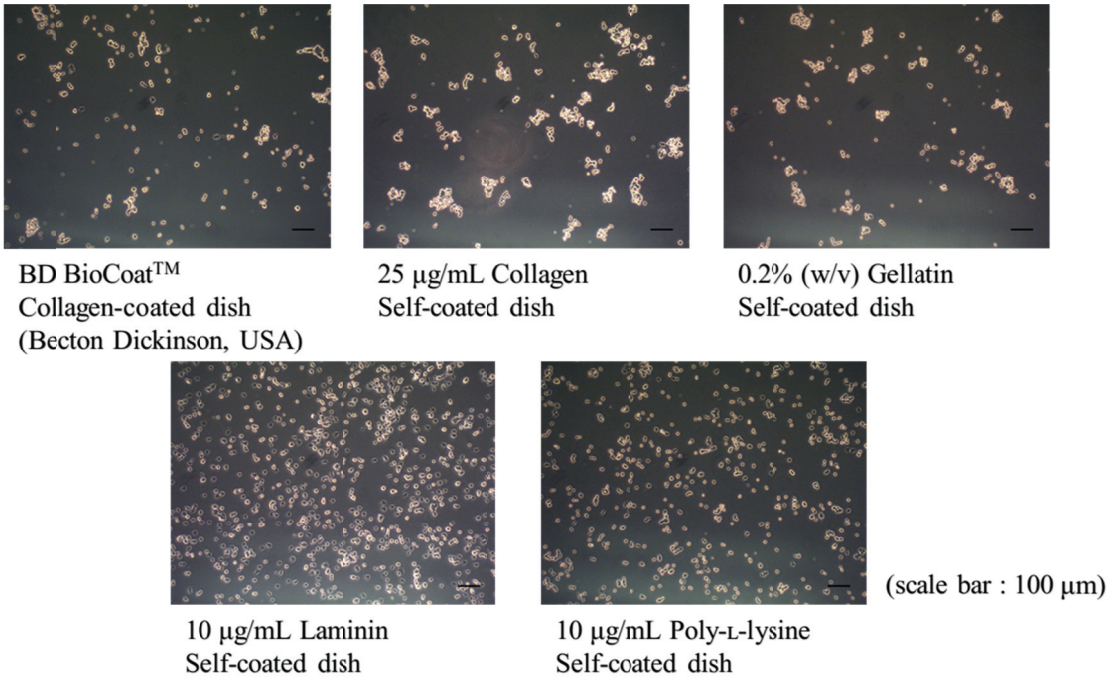

Fig. 2 Optimization of surface-coating substrates of cell culture dishes for PC12

Five types of substrates were considered for optimal cultivation of PC12 cells to achieve firm attachment to the dish surface and maintenance of the single-cell state of the cells.

Analysis of the total fluorescence intensity of the injected solution showed that it increased proportionally to the injection volume, implying accurate control of injection volume by the microinjector (Fig. 3). The total neurite length of the cells injected with Texas Red solution showed no significant difference from that of the control cells without injection (Fig. 4), indicating that there was no significant physical effect of microinjection on cell conditions.

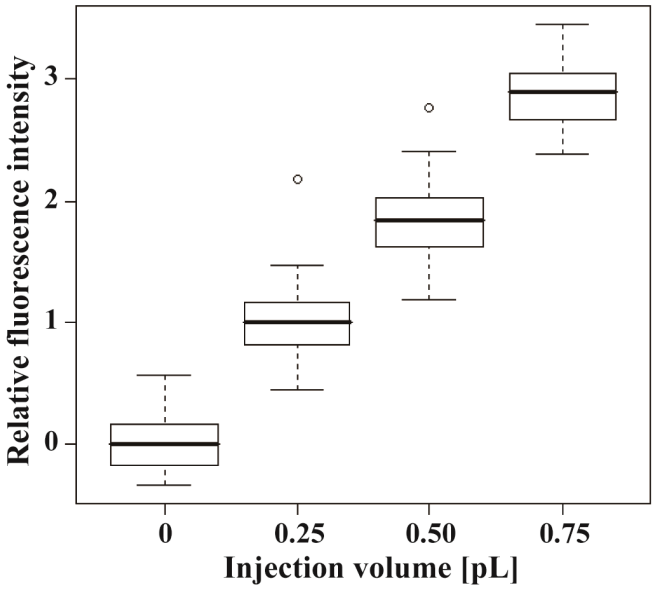

Fig. 3 Confirmation of injection volume control by the CI-2500 microinjector

Fluorescence intensity of each injection volume was normalized to the fluorescence intensity at 0.25 pL.

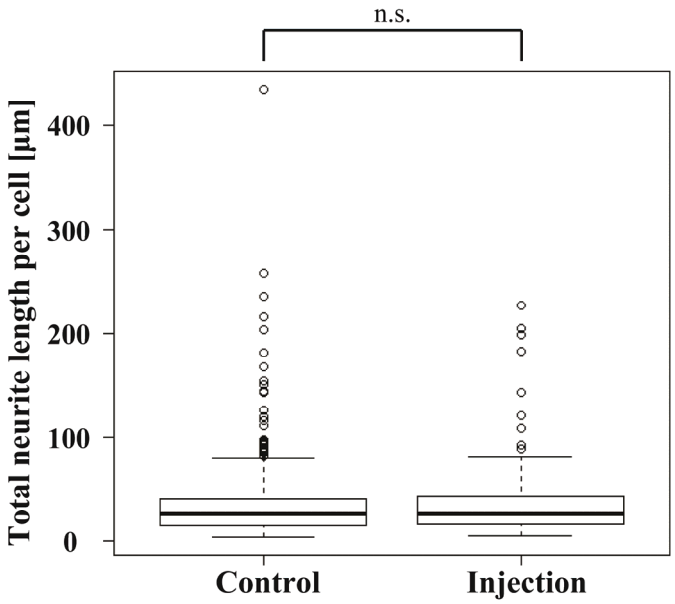

Fig. 4 Confirmation of the possible influence of capillary penetration on PC12 differentiation

Upper fence of each whisker was determined by the value 1.5 IQR above the third quartile, IQR standing for inter quartile range, which represents the range between the first quartile and the third quartile. A total of 397 control cells and 112 cells injected with Texas Red solution were analyzed. The number of outliers was 31 and 9 in the "Control" and "Injection" group, respectively. The data sets showed no statistically significant difference based on the Mann–Whitney *U* test (*P*=0.54, n.s., not significant).

Single-cell analysis of PC12 differentiation inhibition by U0126

Changes in the distribution of the neurite length suggested that PC12 differentiation was successfully inhibited by direct injection of U0126 in a dose-dependent manner (distribution of dots in Fig. 5). The direct injection method also enabled more accurate quantification of the inhibitor introduced into each target cell. On average, injection of 1.5×10^7 U0126 molecules per target cell resulted in a 59% decrease in the neurite length (solid line in Fig. 5).

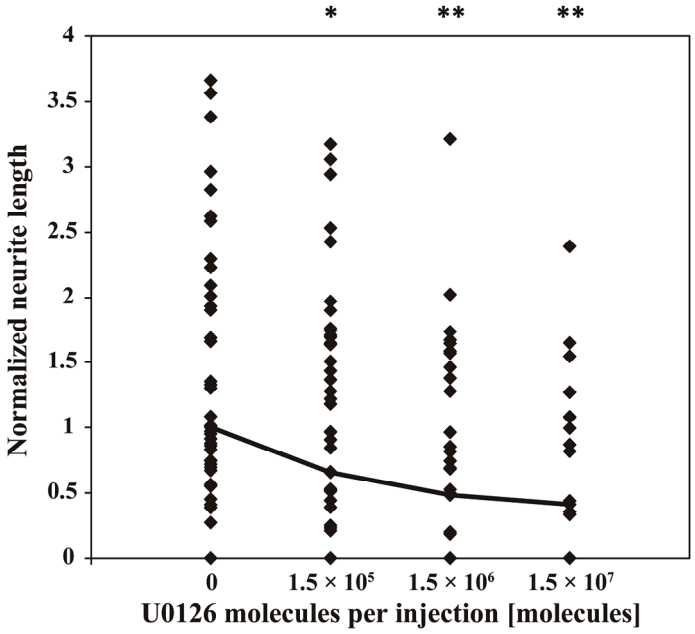

Fig. 5 Quantification of the total neurite length of PC12 cells injected with U0126

Each data point represents the neurite length of each target cell, and the solid line represents the average neurite length across all analyzed cells. Kruskal-Wallis test followed by Shirley-Williams test indicated that the inhibitive effect of U0126 injection was statistically significant (95% confidence interval for 1.5×10^5 molecules per injection, 99% confidence interval for 1.5×10^6 and 1.5×10^7 molecules per injection).

However, when U0126 was simply added to the culture medium as the existing method, the lower limit of U0126 quantity for inhibition of PC12 differentiation was 0.1 μM, which can be calculated as 1.2×10^8 molecules per cell (Fig. 6). The inhibitive effect of U0126 when added at a lower quantity was confirmed as statistically insignificant by single-factor one-way ANOVA (P=0.21). This result indicated that direct injection enabled more accurate and elaborate control of U0126 introduction compared to existing methods, even when lower quantity of the inhibitor was used.

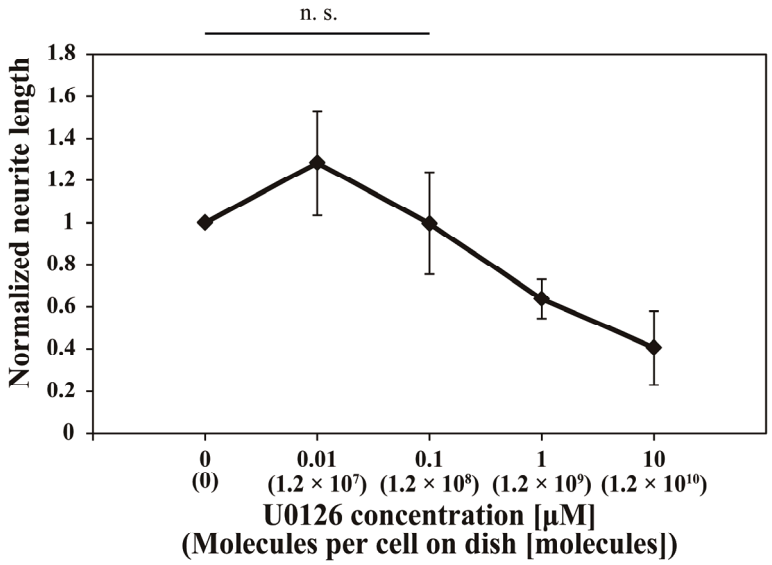

Fig. 6 Quantification of the total neurite length of PC12 cells cultured in U0126-containing culture medium

Average neurite length of 200–400 cells was represented as a normalized value. Single-factor one-way ANOVA was performed for confirmation of statistical significance (error bar: ±SD, P=0.21, n.s., not significant).

Use of the single-cell microinjection technique combined with Celltracker^{TM} staining enabled a long-term time-course observation of individual target cells that had been injected with U0126 (Fig.1 and Fig. 7). Time-course changes in neurite length of each fluorescent cell showed that cells injected with a smaller number of U0126 molecules extended long neurites faster than cells injected with a larger number of U0126 molecules (Fig. 7). In contrast, a number of cells that were injected with a larger amount of U0126 showed no detectable neurite outgrowth (represented by thicker black lines in Fig. 7, overlapping with the *X*-axis; see figure legends for details). Moreover, neurite length of each target cell showed dynamic changes that were largely variable, even amongst the cells treated under the same conditions (Fig. 7). Each line graph showed a dynamic pattern of time-course change, indicating that the change in neurite length of each cell was not a one-way process that involved only "growing" of the neurites. Instead, this result implied that neurite outgrowth, as a phenotypic change in the neuronal differentiation process, is a dynamic phenomenon that is highly variable across individual cells (Fig. 7).

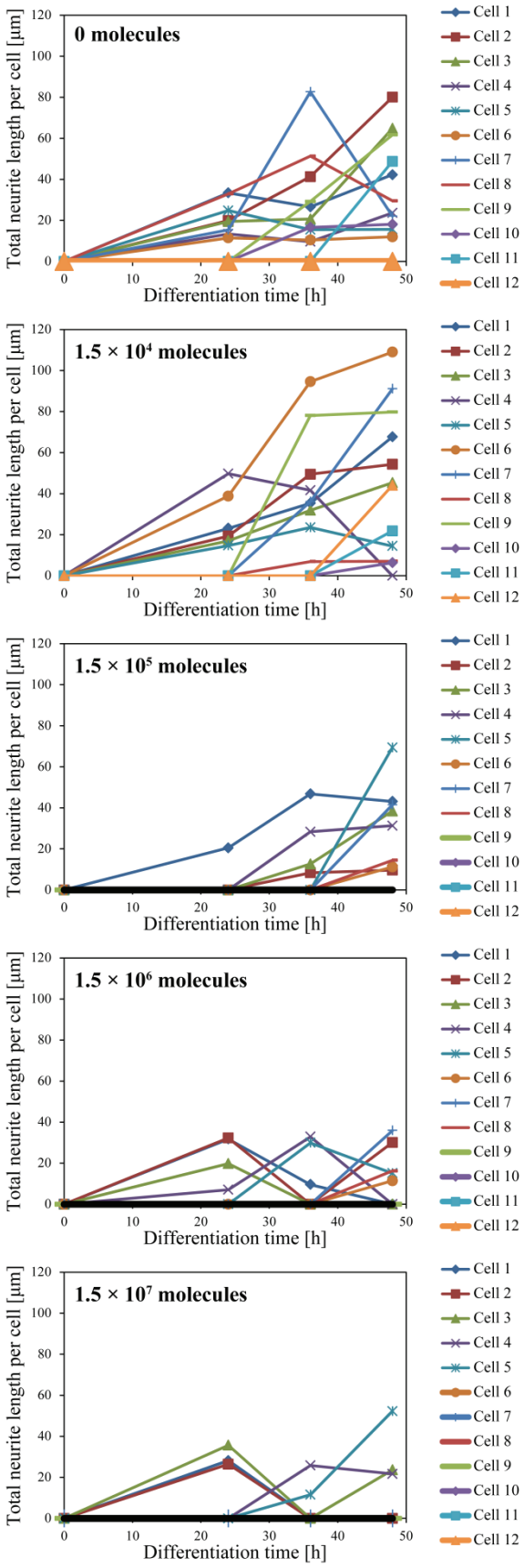

Fig. 7 Dynamic changes in total neurite length of 12 individual target cells analyzed at the single cell level during the PC12 neuronal differentiation process

Individual lines represent the time-course change in total neurite length of individual target cells. Thicker black lines that are overlapping with the *X*-axis represent the cells that did not have detectable neurite outgrowth over time. In graphs for 1.5×10^5 and 1.5×10^6 molecules, the thicker black line on the *X*-axis represents Cell 9, Cell 10, Cell 11, and Cell 12, overlapping together. In the graph for 1.5×10^7 molecules, the thicker black line represents Cell 6 through Cell 12. The number of U0126 molecules injected in each cell is indicated in the upper left of each graph.

Discussion

In this study, we described a strategy of combining single-cell analysis with direct microinjection technique to enable accurate regulation of chemical agent introduced into individual target cells and quantitative analysis of the outcomes.

U0126 is a well-known inhibitor for MEK, and it has been known to suppress the neuronal differentiation of PC12 cells (22). However, generally, it has been used in the form of an additive to culture medium at concentrations usually higher than the order of 1 μM (22, 25, 26). Indeed, U0126 concentration that is lower than 0.1 μM proved unsuitable for inhibition of PC12 differentiation (Fig. 6). It can be considered that a larger quantity of U0126 in the culture medium surrounding PC12 cells is necessary in order for the inhibitor to acquire sufficient driving force to enter into the target cells. However, by using the direct injection method, we successfully introduced smaller quantity of U0126 into individual target cells in a precisely controlled manner. PC12 differentiation was clearly suppressed when 1.5×10^7 molecules were injected per each cell (59% compared to control, Fig. 5), which is an amount that is approximately comparable to 0.01 μM in culture medium. This result indicates that we had successfully inhibited PC12 differentiation by using lower amount of U0126 compared with existing methods, without being affected by the surrounding environment of target cells. This is a novel attempt to examine the quantitative relationship between the amount of inhibitor actually introduced into each cell and the inhibitive effect on phenotypic changes of individual differentiated cells.

Moreover, single-cell analysis of differentiating PC12 cells enabled accurate observation of changes on target cell phenotype that occur during the process. Time-course observations of the pattern of neurite length changes showed that neuronal differentiation of PC12 accompanied dynamic changes that were largely variable among individual target cells (Fig. 7). Considering the observed heterogeneity in differentiation of the cell population cultured under the same conditions, it is important to regulate and analyze the changes that each cell undergoes at the single cell level. Combined with techniques that accurately measure the initial condition of individual target cells, the microinjection technique can be a powerful tool for single-cell regulation and time-course analysis at the single cell level.

Summary

Experimental methods that have been conventionally used for inhibition of PC12 neuronal differentiation mainly involved adding cell-permeable chemical inhibitors to the cell culture medium and analyzing the outcomes as averaged figures obtained from thousands of target cells. However, by simply adding the inhibitors to the cell culture medium, it is impossible to accurately regulate the quantity that is actually introduced into individual target cells. Moreover, recent studies based on single-cell analysis have shown the genomic and phenotypic differences among individual cells in the same population cultured and treated under identical conditions. To solve the problems of conventional experimental methods of bulk analysis, quantitative inhibition of the NGF-induced differentiation of PC12 cells was attempted by directly introducing U0126 molecules into individual target cells using the automated microinjection system. By optimizing the conditions for PC12 cell culture and microinjection into the target cells, efficient introduction of the differentiation-inhibiting agent into each single cell could be performed in a quantitative and direct manner. By using this method, PC12 differentiation was successfully inhibited with lower amount of U0126 compared with existing methods of simply adding the chemical to the culture medium, without being affected by the surrounding environment of target cells. Furthermore, combining the direct microinjection method with fluorescence labeling of the target cells enabled long-term time-course observation of the phenotypic changes that occur on individual cells at the single cell level. These results indicated that the changes in neurite length of each cell undergoing neuronal differentiation was not a one-way process that involved only “growing” of the neurites, but a dynamic bidirectional phenomenon that is highly variable across individual cells. This chapter highlights the effectiveness of direct microinjection method for rigorous control of the amount of differentiation-regulating factors introduced into individual target cells and analysis of the outcomes at the single cell level.

References

1. **Pankow S, Bamberger C, Klippel A, Werner S.** 2006. Regulation of epidermal homeostasis and repair by phosphoinositide 3-kinase. J Cell Sci **119:**4033-4046.
2. **Barker N, van Es JH, Kuipers J, Kujala P, van den Born M, Cozijnsen M, Haegebarth A, Korving J, Begthel H, Peters PJ, Clevers H.** 2007. Identification of stem cells in small intestine and colon by marker gene Lgr5. Nature **449:**1003-1007.
3. **Dow LE, O'Rourke KP, Simon J, Tschaharganeh DF, van Es JH, Clevers H, Lowe SW.** 2015. Apc restoration promotes cellular differentiation and reestablishes crypt homeostasis in colorectal cancer. Cell **161:**1539-1552.
4. **Johansson CB, Svensson M, Wallstedt L, Janson AM, Frisen J.** 1999. Neural stem cells in the adult human brain. Exp Cell Res **253:**733-736.
5. **Lee H, Lee YJ, Choi H, Ko EH, Kim JW.** 2009. Reactive oxygen species facilitate adipocyte differentiation by accelerating mitotic clonal expansion. J Biol Chem **284:**10601-10609.
6. **Dor Y, Glaser B.** 2013. Beta-cell dedifferentiation and type 2 diabetes. N Engl J Med **368:**572-573.
7. **Huangfu D, Maehr R, Guo W, Eijkelenboom A, Snitow M, Chen AE, Melton DA.** 2008. Induction of pluripotent stem cells by defined factors is greatly improved by small-molecule compounds. Nat Biotechnol **26:**795-797.
8. **Okita K, Nakagawa M, Hyenjong H, Ichisaka T, Yamanaka S.** 2008. Generation of mouse induced pluripotent stem cells without viral vectors. Science **322:**949-953.
9. **Zhou H, Wu S, Joo JY, Zhu S, Han DW, Lin T, Trauger S, Bien G, Yao S, Zhu Y, Siuzdak G, Scholer HR, Duan L, Ding S.** 2009. Generation of induced pluripotent stem cells using recombinant proteins. Cell Stem Cell **4:**381-384.

10. **Ieda M, Fu JD, Delgado-Olguin P, Vedantham V, Hayashi Y, Bruneau BG, Srivastava D.** 2010. Direct reprogramming of fibroblasts into functional cardiomyocytes by defined factors. Cell **142:**375-386.

11. **Wang D, Bodovitz S.** 2010. Single cell analysis: the new frontier in 'omics'. Trends Biotechnol **28:**281-290.

12. **Kelbauskas L, Ashili SP, Houkal J, Smith D, Mohammadreza A, Lee KB, Forrester J, Kumar A, Anis YH, Paulson TG, Youngbull CA, Tian Y, Holl MR, Johnson RH, Meldrum DR.** 2012. Method for physiologic phenotype characterization at the single-cell level in non-interacting and interacting cells. J Biomed Opt **17:**037008.

13. **Konry T, Golberg A, Yarmush M.** 2013. Live single cell functional phenotyping in droplet nano-liter reactors. Sci Rep **3:**3179.

14. **Smith ZD, Nachman I, Regev A, Meissner A.** 2010. Dynamic single-cell imaging of direct reprogramming reveals an early specifying event. Nat Biotechnol **28:**521-526.

15. **Narsinh KH, Sun N, Sanchez-Freire V, Lee AS, Almeida P, Hu S, Jan T, Wilson KD, Leong D, Rosenberg J, Yao M, Robbins RC, Wu JC.** 2011. Single cell transcriptional profiling reveals heterogeneity of human induced pluripotent stem cells. J Clin Invest **121:**1217-1221.

16. **Gerlach C, Rohr JC, Perie L, van Rooij N, van Heijst JW, Velds A, Urbanus J, Naik SH, Jacobs H, Beltman JB, de Boer RJ, Schumacher TN.** 2013. Heterogeneous differentiation patterns of individual CD8+ T cells. Science **340:**635-639.

17. **Brambrink T, Foreman R, Welstead GG, Lengner CJ, Wernig M, Suh H, Jaenisch R.** 2008. Sequential expression of pluripotency markers during direct reprogramming of mouse somatic cells. Cell Stem Cell **2:**151-159.

18. **Greene LA, Tischler AS.** 1976. Establishment of a noradrenergic clonal line of rat

adrenal pheochromocytoma cells which respond to nerve growth factor. Proc Natl Acad Sci USA **73:**2424-2428.

19. **Fox JH, Barber DS, Singh B, Zucker B, Swindell MK, Norflus F, Buzescu R, Chopra R, Ferrante RJ, Kazantsev A, Hersch SM.** 2004. Cystamine increases L-cysteine levels in Huntington's disease transgenic mouse brain and in a PC12 model of polyglutamine aggregation. J Neurochem **91:**413-422.

20. **Johnson G, Refolo LM, Wallace W.** 1993. Heat-shocked neuronal PC12 cells reveal Alzheimer's disease-associated alterations in amyloid precursor protein and tau. Ann N Y Acad Sci **695:**194-197.

21. **Lachyankar MB, Sultana N, Schonhoff CM, Mitra P, Poluha W, Lambert S, Quesenberry PJ, Litofsky NS, Recht LD, Nabi R, Miller SJ, Ohta S, Neel BG, Ross AH.** 2000. A role for nuclear PTEN in neuronal differentiation. J Neurosci **20:**1404-1413.

22. **Das KP, Freudenrich TM, Mundy WR.** 2004. Assessment of PC12 cell differentiation and neurite growth: a comparison of morphological and neurochemical measures. Neurotoxicol Teratol **26:**397-406.

23. **Youoku S, Suto Y, Ando M, Akiolto.** 2007. Automated microinjection system for adherent cells - art. no. 66330S. Biophotonics 2007: Optics in Life Science **6633:**S6330-S6330.

24. **Williams DA.** 1986. A note on Shirley's nonparametric test for comparing several dose levels with a zero-dose control. Biometrics **42:**183-186.

25. **Favata MF, Horiuchi KY, Manos EJ, Daulerio AJ, Stradley DA, Feeser WS, Van Dyk DE, Pitts WJ, Earl RA, Hobbs F, Copeland RA, Magolda RL, Scherle PA, Trzaskos JM.** 1998. Identification of a novel inhibitor of mitogen-activated protein

kinase kinase. J Biol Chem **273:**18623-18632.

26. **Ferrari A, Faraci P, Cecchini M, Beltram F.** 2010. The effect of alternative neuronal differentiation pathways on PC12 cell adhesion and neurite alignment to nanogratings. Biomaterials **31:**2565-2573.

Chapter II Study on cellular changes induced by co-culture of normal HEK293T cells with *Scribble* knockout cells

Cancer, being one of the leading causes of death in Japan, is known to involve progressive dysregulation of the cellular differentiation state along the outset and development of the disease. As cancer progresses, cells lose the expression of tissue or organ-specific marker genes and undergo unregulated cell division. Clinical studies have also revealed that the differentiation state of cancer cells is related to the metastatic ability and prognosis of cancer (1, 2). Molecular biological research on various types of cancers has led to the identification of numerous oncogenes and tumor suppressor genes that are involved in the cancer development process. Many of these genes are known to function during cellular activities including cell cycle control, DNA repair, apoptosis, etc. These identified genes have been utilized in cancer therapy as targets for drug development or markers for diagnosis. Research for cancer control has mainly focused on the genetic transformations in cancer cells themselves and the changes that occur in the cells when they obtain certain cancer-related transformations.

However, the fact that cancer cells are surrounded by normal cells in an organism has not been the main emphasis of cancer research. In the very early stages of cancer development, cancer-associated gene transformation occurs at the single cell level, and the disease then progresses as the cell grows and obtains additional gene transformations. Cells harboring these gene transformations are present in a microenvironment in which they must compete with the surrounding normal cells, which exist in much larger numbers, for survival. Recently, several studies using *Drosophila melanogaster* or mammalian cell cultures showed that when cells with cancer-related gene transformation are co-cultured with normal cells, an interaction occurs between the two types of cells, resulting in elimination from the cell layer or apoptosis of one of the cell types that has been outcompeted by the other (3-5). One of the examples of the genetic transformations that induce intercellular interactions between transformed and normal cells is the loss of the *Scribble* gene. *Scribble* is a well-known tumor suppressor gene that is involved in epithelial cell polarity and proliferative control (6). *Scribble* has been shown to behave as a tumor suppressor in mice (7); in addition, the expression of this gene has been shown to be decreased in human cancers, such as colon and breast cancers (8, 9). In *in vivo* experiments

using *D. melanogaster* and an *in vitro* co-culture system using a dog-derived epithelial cell line, cells with decreased *Scribble* expression have been shown to be eliminated from the epithelial cell layer when surrounded by a larger number of normal cells (5, 10). However, to date, the cellular changes that occur when human-derived cells bearing *Scribble* mutations are co-cultured with normal cells have not yet been elucidated. Moreover, to understand the underlying processes and to effectively take advantage of the molecules that play critical roles, the molecular mechanism of mutual recognition and interaction between transformed and normal cells must be clarified in detail.

In this chapter, we constructed a co-culture system of *Scribble* knockout and normal cells using the human embryonic kidney (HEK293T) cell line, and investigated the changes that the cells underwent by analyzing time-course microscopic images of the co-culture. Moreover, we attempted to elucidate the molecular changes that occured in these cells by seperating each cell type from the co-culture system by fluorescence-activated cell sorting (FACS) and by performing proteome analysis using the whole protein extracted from the cells. Considering this interaction between cancer-related transformed and surrounding normal cells, it can be expected that a completely new apporach toward cancer control, such as exploiting surrounding cells to attack newly arising cancer cells, can become possible.

Materials and Methods

Plasmids and antibodies

To construct the CRISPR/Cas9 system for *Scribble* knockout in HEK293T cells, pCas-Guide plasmid (Origene, USA) was amplified by polymerase chain reaction (PCR) using oligonucleotides 5′-GTTTTAGAGCTAGAAATAGCAAGTTAAAATAAGGC-3′ and 5′-CG ATCCCGCGTCCTTTCCAC-3′. Annealed oligonucleotide including the guide RNA sequence to target *Scribble* in HEK293T cells (Forward: 5′-AAGGACGCGGGATCGGTGGCGCTGCA ACCGGCACGGTTTTAGAGCTAGAA-3′ and Reverse: 5′-TTCTAGCTCTAAAACCGTGCC GGTTGCAGCGCCACCGATCCCGCGTCCTT-3′) was cloned into the amplified pCas-Guide using the In-Fusion HD Cloning Kit (Clontech, USA), resulting in pCas-Guide/hSCRIB. Left

(LHR) and right homologous regions (RHR) to induce homologous recombination following the double-strand break of *Scribble* were cloned from the genomic DNA of HEK293T cells, and inserted into HR410PA-1 plasmid (System Biosciences, USA). Genomic DNA was extracted from wild type HEK293T cells using the GenElute Mammalian Genomic DNA Miniprep Kit (Sigma, USA), according to the manufacturer's protocol. The LHR was amplified from the extracted genomic DNA by PCR using oligonucleotides 5′-GACGGCCAGTGAATTGAGACC TGGGCAGGGGGTTG-3′ and 5′-TTGAGTGGAAAGATCCTTGAGCATGGTGCGGGTGG -3′, and cloned into *Eco*RI and *Bgl*II sites of HR410PA-1. The RHR was amplified using oligonucleotides 5′-TCGGATCCCCGTCGAGAGTCGGTGGACAAGCGGCAC-3′ and 5′-AT TACGCCAAGCTTGCAAGAACTCAGTAAACGCTCCCCACA-3′, and cloned into *Sal*I and *Sph*I sites of HR410PA-1 into which the LHR has already been cloned. The resulting donor plasmid was designated HR410PA-1/hSCRIB.

A mouse monoclonal antibody against glyceraldehyde-3-phosphate dehydrogenase (GAPDH), clone 6C5 (MAB374, Millipore, USA) was used at a dilution of 1:500 for western blot analysis. Horseradish peroxidase (HRP)-conjugated anti-mouse immunoglobulin G (IgG) (NA931, GE Healthcare, USA) was used at a dilution of 1:5,000 as the secondary antibody for the detection of GAPDH. A goat polyclonal antibody against Scribble, clone K-21 (sc-11048, Santa Cruz Biotechnology, USA) was used at a dilution of 1:200 for the detection of Scribble protein production by western blot analysis. As the secondary antibody for the detection of Scribble, HRP-conjugated anti-goat IgG (sc-2020, Santa Cruz Biotechnology, USA) was used at a dilution of 1:5,000.

Cell culture and establishment of strains

HEK293T cells (RCB2202, RIKEN Cell Bank, Japan) were cultured in Dulbecco's modified Eagle's medium (DMEM, Nacalai Tesque, Japan) supplemented with 10% (v/v) fetal bovine serum (FBS, Gibco, USA). For maintenance of the HEK293T cells, 1.0×10^6 cells were seeded on 100 mm dishes and incubated at 37°C in a humidified atmosphere with 95% air and 5% CO_2. Culture medium was replaced every 2–3 days, and the cells were passaged every 4–5 days.

To establish the *Scribble* knockout cell line, HEK293T cells were transfected with both pCas-Guide/hSCRIB and HR410PA-1/hSCRIB plasmids using X-tremeGENE HP DNA

Transfection Reagent (Roche, Switzerland), according to the manufacturer's protocol. To establish the negative control cell line that is GFP^+ but has a normal level of *Scribble* expression, HEK293T cells were transfected with only HR410PA-1/hSCRIB plasmid. In both cases, 2 μg of total plasmid and 6 μL of the transfection reagent were used for each well of 6-well cell culture plates. Transfection of the cells was followed by selection in culture medium containing puromycin at a final concentration of 1 μg/mL. All selected cells were further maintained in culture medium containing 1μg/mL of puromycin.

Sample preparation for western blot analysis

Whole protein was extracted from normal or *Scribble* knockout HEK293T cells for the detection of target proteins by western blot analysis. Cells were seeded onto 6-well plates at 5.0 × 10^5 cells per well and cultured for 48 h before protein extraction. Cell culture supernatant was removed from each well and the cells were washed twice with ice-cold 1× phosphate buffered saline (PBS, 137 mM NaCl, 8.1 mM Na_2HPO_4, 2.68 mM KCl, 1.47 mM KH_2PO_4, pH7.4, NIPPON GENE, Japan). Following the addition of 150 μL RIPA buffer [50 mM Tris-HCl pH8.0, 150 mM NaCl, 0.5% (w/v) sodium deoxycholate, 0.1% (w/v) sodium dodecyl sulfate (SDS), 1.0% (w/v) NP-40 substitute, Wako, Japan] containing 1% (v/v) protease inhibitor cocktail for mammalian cells (Sigma, USA) to each well, the cells were scraped off from the dish surface using cell scrapers (Iwaki, Japan). After homogenization of the cell suspension by thoroughly pipetting the solution 20–30 times, it was moved to a new 1.5 mL tube and incubated on ice for over 5 min. Cell lysates were centrifuged at 14,000 × g at 4°C for 20 min and the supernatant was moved to a clean 1.5 mL tube as the whole protein extract. Protein concentration was measured using the Bicinchoninate Protein Assay kit (Nacalai Tesque, Japan) and the same amount of protein from each sample was applied to SDS-PAGE and western blot analysis.

Time course observation of the co-cultures

Wild-type and *Scribble* knockout HEK293T cells (KO#18 strain) or cells transfected only with the donor (HR410PA-1/hSCRIB) plasmid (D#1 strain) were mixed in a ratio of 9:1 (4.5×10^5:5.0×10^4) and seeded on 35 mm glass base dishes with cover glasses of thickness 0.12–0.17 mm (Iwaki, Japan) (Fig. 1). Microscopic observation of a fixed area on each

co-culture dish was performed at the indicated time points, using the microscope that is attached to the microinjector CI-2500 (Fujitsu Ltd., Japan). To detect the green fluorescence of GFP, the fluorescence filter set with a 460–495 nm excitation filter, a 510 IF emission filter and a 505 nm dichroic mirror (U-MWIB3, Olympus, Japan) was used. The size of each microscopic field was 200 μm × 200 μm and 64 images were obtained for each dish, meaning that an area of size 1.6 mm × 1.6 mm was fixed for observation on each co-culture dish (Fig. 1). The number of GFP^+ cells in all obtained images was counted and the time-course change in the numbers was analyzed.

Sample preparation for proteome analysis

Wild-type and KO#18 or D#1 cells were mixed in a ratio of 9:1 (3.6×10^6:4.0×10^5) and seeded on 100 mm plastic dishes (Fig. 1). After 90 h of incubation, cells were detached from the dishes by treatment with 1.25 g/L-Trypsin/0.5 mmol/L-EDTA solution (Nacalai Tesque, Japan). Detached cells were suspended in 10 mL of growth medium and subjected to cell sorting by flow cytometry. Wild-type (GFP^-) cells and KO#18 or D#1 (GFP^+) cells were separated by FACS (JSAN, Bay bioscience, Japan) (Fig. 1). Whole protein was extracted from each type of cell as described previously (11, 12). Cells were resuspended in 1 mL of lysis buffer [100 mM dithiothreitol and 4% (w/v) SDS in 100 mM Tris-HCl, pH7.5] and incubated at 95°C for 5 min. Cell lysates were sonicated on ice using the Bioruptor UCD-250T (Cosmo Bio, Japan) at 250 W with 15-s on-and-off cycles for 10 min. The solution was centrifuged (16,100 × *g* at 4°C for 10 min) and the supernatant was collected into a new 1.5 mL tube. Collected samples were subjected to ultrafiltration with Amicon Ultra-0.5 centrifugal filter units (10 kDa, Millipore, USA) and buffer-exchanged with 200 mM triethyl ammonium bicarbonate (TEAB, Sigma, USA). Proteins were reduced by adding Tris (2-carboxyethyl) phosphine to a final concentration of 10 mM and incubating at 55°C for 90 min. Following the incubation, 25 μL of iodoacetamide (375 mM) was added and the reaction solution was incubated for 45 min at room temperature, protected from light. Acetone precipitation of the proteins was performed by adding 1 mL of ice-cold acetone and incubating at −20°C for 3 h. The precipitated proteins were resuspended with 250 μL of 200 mM TEAB to proceed to tryptic digestion. To the protein solution, 2 μL of sequencing grade modified trypsin (1 μg/μL, Promega, USA) was added and the reaction solutions were incubated overnight (18 h) at 37°C.

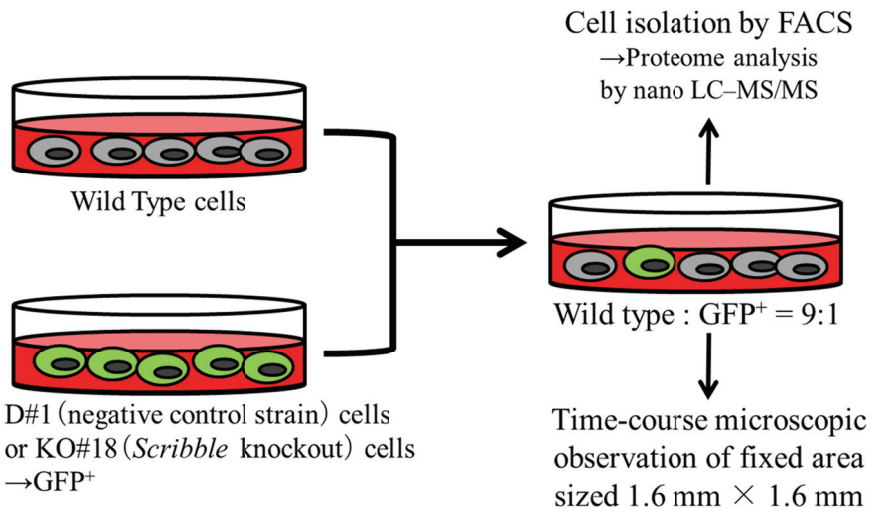

Fig. 1 Schematic diagram of the procedure of co-culture experiments

LC–MS/MS analysis

Proteome analysis was performed using an LC–MS/MS (Ultimate 3000, Thermo Fisher Scientific, USA; LTQ Velos Mass Spectrometer, Thermo Fisher Scientific, USA) system equipped with a long monolithic silica capillary column, as previously described (13). A monolithic silica capillary column was prepared from a mixture of tetramethoxysilane and methyltrimethoxysilane (14). Tryptic digests were separated by reverse-phase chromatography using a monolithic silica capillary column (200 cm in length, 0.1-mm inner diameter), at a flow rate of 500 nL/min. A gradient was achieved by changing the ratio of the two eluents: eluent A, 0.1% (v/v) formic acid and eluent B, 80% acetonitrile containing 0.1% (v/v) formic acid. The gradient started with 5% B, increased to 45% B for 600 min, further increased to 95% B to wash the column for 140 min, returned to the initial condition and was held for re-equilibration of the column. The separated analytes were detected using a mass spectrometer with a full scan range of 350–1,500 m/z, followed by seven data-dependent collision-induced dissociation (CID) MS/MS scans. Electrospray ionization (ESI) voltage was set at 2.4 kV. The collected data were reviewed for protein identification. Blank runs were inserted between runs of different samples.

Proteome data analysis

Proteome data were analyzed using Proteome Discoverer 1.4 (Thermo Fisher Scientific, USA). Protein identification was performed using the Mascot algorithm against the protein database (20,193 sequences) from Swiss-Prot (https://www.uniprot.org/), with a precursor mass tolerance of 2.3 Da and a fragment ion mass tolerance of 0.8 Da. The carbamidomethylation of cysteine was set as a fixed modification for qualitative proteome analysis. The data were then filtered with a cut-off criteria of q value $\leq$ 0.01, corresponding to a 1% false discovery rate (FDR) on a spectral level. Gene ontology analysis of the identified proteins was performed based on the Database for Annotation, Visualization and Integrated Discovery (DAVID, https://david.ncifcrf.gov) (15, 16), using the UniProt accession database as the identifier.

Results

Establishment of* Scribble *knockout HEK293T strains

To construct a co-culture system of cells bearing cancer-related transformation and normal cells, the tumor suppressor gene *Scribble* was knocked out in HEK293T cells using the CRISPR/Cas9 system for genome editing (17, 18). Normal production of Scribble protein in cells transfected only with the donor plasmid (D#1 strain) and complete loss in cells transfected with both pCas-Guide/hSCRIB and the donor plasmid (KO#18 strain) was confirmed by western blot analysis (Fig. 2). It was also successfully confirmed that *Scribble* was stably knocked out in KO#18 cells freshly thawed from frozen stocks.

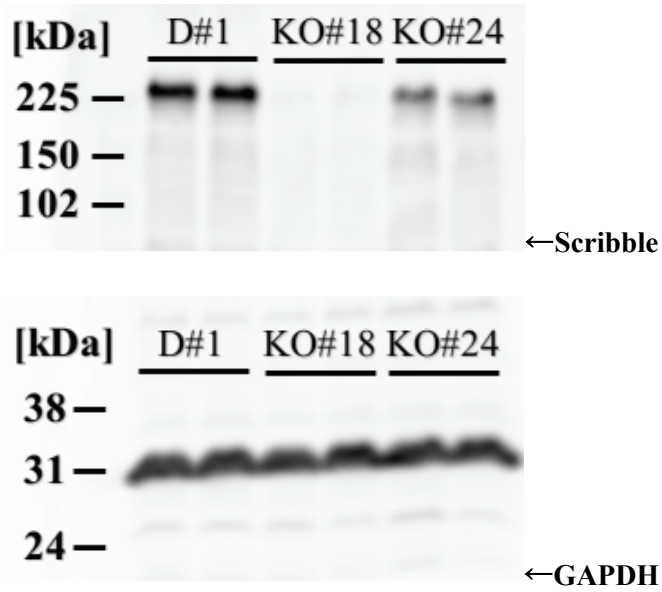

Fig. 2 Confirmation of *Scribble* knockout in HEK293T cells by western blot analysis

Time-course microscopic observation of the co-cultured cells

Proliferation of the *Scribble* knockout cells co-cultured with the normal cells was investigated by analyzing microscopic images of a 1.6 mm × 1.6 mm-sized area on each dish at the indicated time points. To analyze the proliferation rate of particular cells over time, the areas subjected to microscopic observation were fixed during the whole time of time-course analysis (Fig. 3). The number of GFP^+ cells on each co-culture dish was counted and the time-course change in cell number was analyzed (Fig. 4). The results of the experiments performed in triplicate showed that even with the same starting cell numbers, there existed a larger number of KO#18 cells than D#1 cells in the co-culture system with wild-type cells, from as early as 12 h (Tables 1 and 2). All observed areas were shown to be completely covered with cells after 48 h of co-culture, indicating that the number of all cells on each dish were identical under all conditions. Therefore, the results indicated that the proliferation of KO#18 cells when co-cultured with wild-type cells was faster than that of D#1, which was used as the negative control strain.

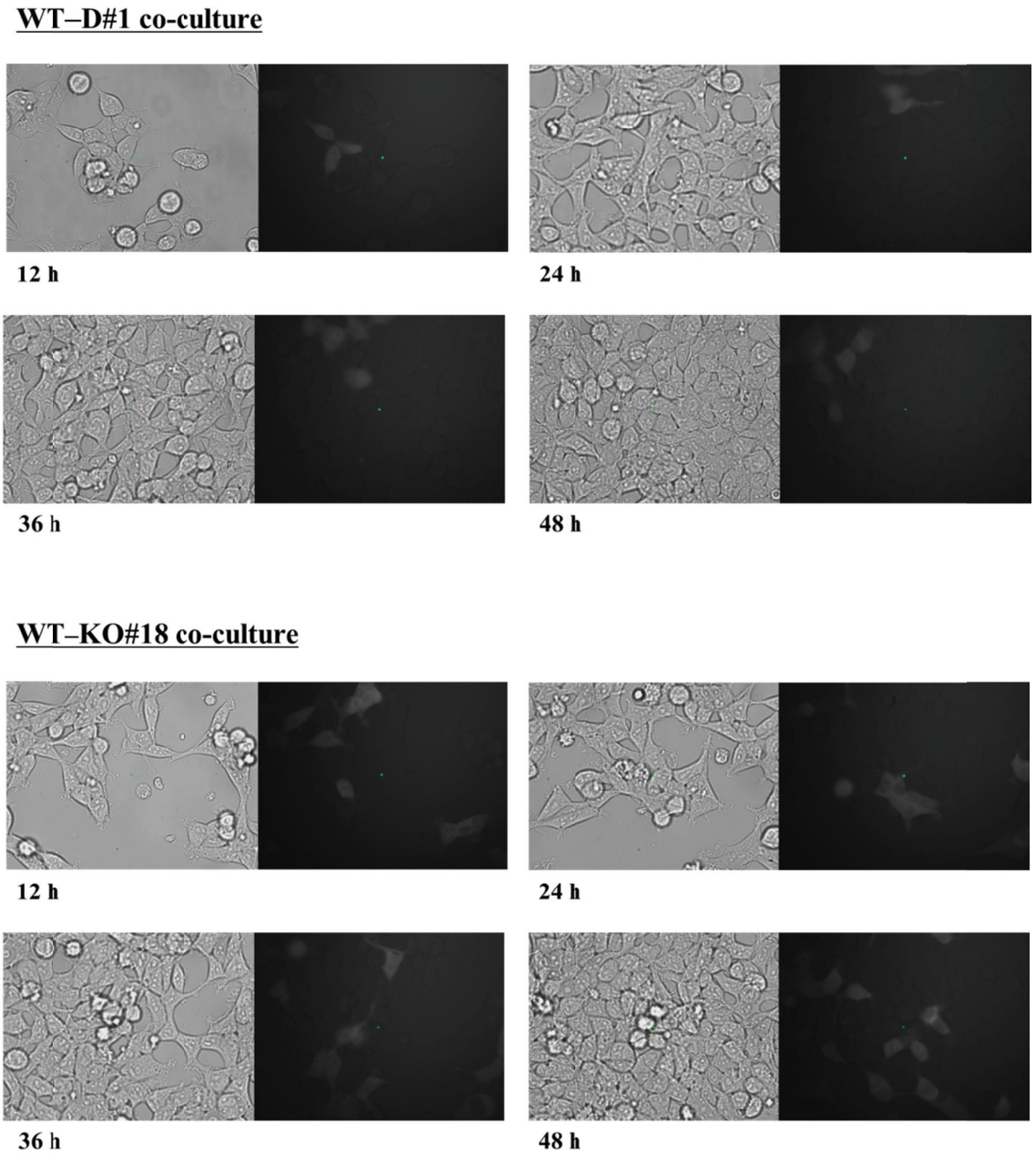

Fig. 3 Time-course microscopic observation of KO#18 or D#1 cells co-cultured with wild-type cells

Representative images from each co-culture dish are shown. The 200 μm × 200 μm-sized area is shown in each microscopic image. GFP^+ cells represent D#1 cells (upper block of images) and KO#18 (lower block of images), respectively.

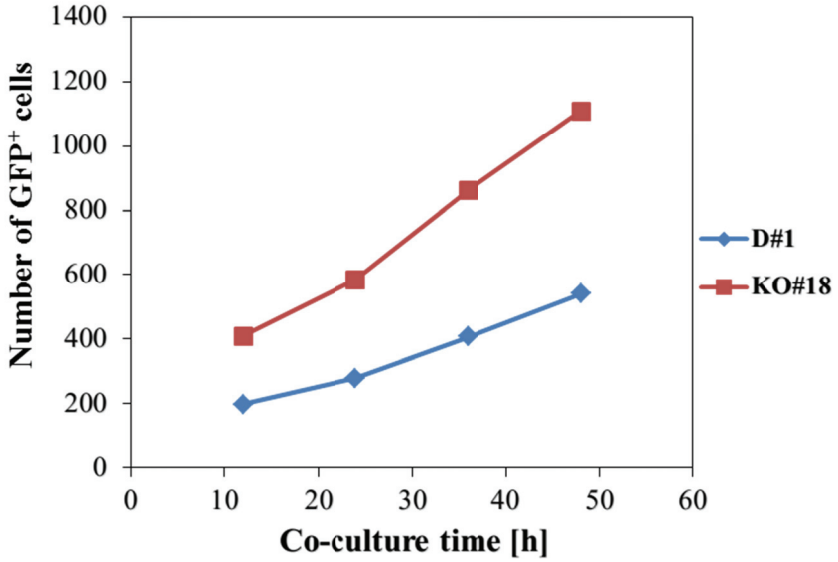

Fig. 4 Time-course changes in the number of GFP$^+$ cells co-cultured with wild-type cells

Table 1 Number of D#1 cells in co-culture with wild-type cells

	12 h	24 h	36 h	48 h
D#1-well 1	233	339	505	645
D#1-well 2	172	232	348	480
D#1-well 3	188	267	367	495
Average	198	279	407	540

Table 2 Number of KO#18 cells in co-culture with wild-type cells

	12 h	24 h	36 h	48 h
KO#18-well 1	467	669	960	1245
KO#18-well 2	300	406	639	832
KO#18-well 3	458	679	987	1251
Average	408	585	862	1109

Proteome analysis of whole protein extracted from co-cultured cells

To investigate the molecular changes that occurred in cells isolated from the co-culture, proteome analysis was performed by nano LC–MS/MS with a long monolithic silica capillary column (200 cm). Cells harvested from co-culture dishes were subjected to cell sorting by FACS, and wild-type cells were separated from GFP^+ cells. Enrichment of each cell type after cell sorting was confirmed by the microscopic observation of GFP fluorescence in the cells. Samples for whole proteome analysis were prepared from the wild-type cells isolated from the co-culture. After tryptic digestion of the protein solutions, peptide concentrations in each sample were measured using the Bicinchoninate Protein Assay kit (Nacalai Tesque, Japan) and the same amount of peptide was used for proteome analysis of all samples.

Mass spectrometry data were used for protein identification based on the Swiss-Prot protein database, which contains more than 20,000 sequences of human proteins. In total, with the cut-off criteria used in this research, 1,124 proteins were identified from the wild-type cells co-cultured with D#1 (negative control) cells and 843 proteins from the wild-type cells co-cultured with KO#18 (*Scribble* knockout) cells (Fig. 5). Among them, 704 proteins were commonly identified from wild-type cells co-cultured with both types of GFP^+ cells. The numbers of proteins that were specifically identified in the co-culture with D#1 cells and KO#18 cells were 420 and 139, respectively. From these results, it could be assumed that the 139 proteins specifically identified from wild-type cells co-cultured with KO#18 cells are involved in the intercellular interaction between normal cells and *Scribble* knockout cells. In this research, further analysis was performed on these proteins.

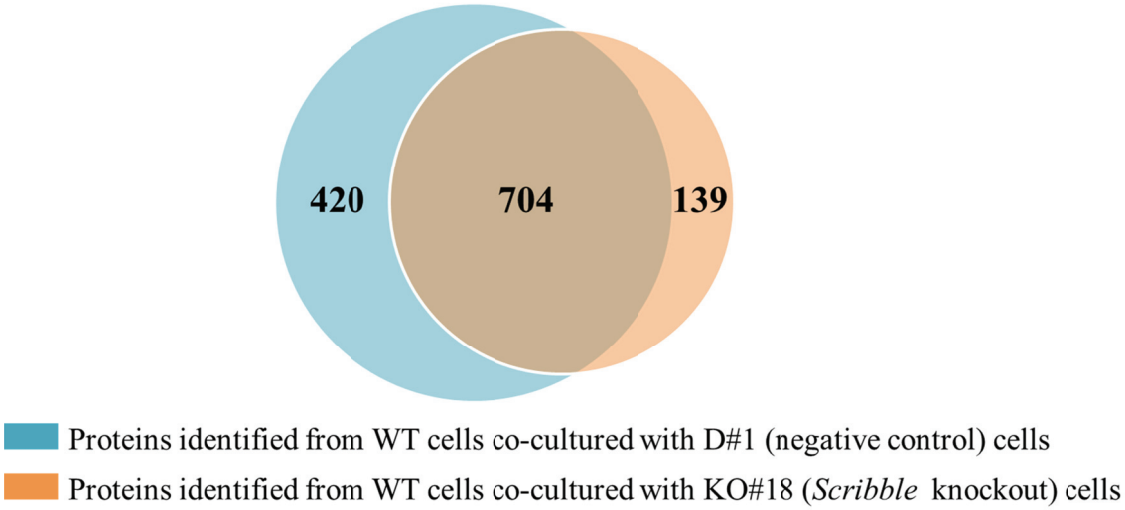

Fig. 5 Protein profiles of wild-type cells co-cultured with either D#1 (negative control) or KO#18 (*Scribble* knockout) cells

Numbers in the Venn diagram indicate the number of proteins identified by qualitative proteome analysis of each sample.

Gene ontology analysis of specifically identified proteins

To investigate the proteins that were uniquely identified from wild-type cells co-cultured with *Scribble* knockout cells in more detail, gene ontology analysis based on the functional annotation tool DAVID (https://david.ncifcrf.gov) (15, 16) was performed. By performing GO analysis of the specifically identified proteins, we attempted to elucidate the characteristic functional group of proteins that is believed to be deeply involved in intercellular interaction between normal and *Scribble* knockout cells. The results showed that among the 139 specifically identified proteins, there were 22 proteins that were annotated to be related to the formation and maintenance of the cytoskeleton in cells (Table 3). Enrichment of the proteins of this category was confirmed by a P value of 2.6×10^{-3} by Fisher's Exact test, which is a statistical test used to determine whether the proportions of components falling into each category differs by group. Among these specifically identified cytoskeleton-related proteins, those that are involved in the formation and maintenance of microtubule structure and functions such as motor activity were also enriched, as indicated by a P value of 1.4×10^{-3}. Proteins such as centromere protein E (accession number Q02224), dynein (Q8IVF4, Q9UFH2), and kinesin family members (Q2VIQ3, Q9BW19) were identified as proteins that are involved in microtubule motor activity.

Table 3 Cytoskeleton-related proteins specifically identified from wild-type cells co-cultured with KO#18 cells

	UniProt Accession number	Gene name	Description
1	P27695	*APEX1*	APEX nuclease (multifunctional DNA repair enzyme) 1
2	O15083	*ERC2*	ELKS/RAB6-interacting/CAST family member 2
3	O75592	*MYCBP2*	MYC binding protein 2
4	Q9Y6W5	*WASF2*	WAS protein family, member 2
5	P35222	*CTNNB1*	Catenin (cadherin-associated protein), beta 1, 88 kDa
6	Q02224	*CENPE*	Centromere protein E, 312 kDa
7	Q8IVF4	*DNAH10*	Dynein, axonemal, heavy chain 10
8	Q9UFH2	*DNAH17*	Dynein, axonemal, heavy chain 17
9	P06396	*GSN*	Gelsolin (amyloidosis, Finnish type)
10	Q9NQX3	*GPHN*	Gephyrin
11	P02533	*KRT14*	Keratin 14
12	P08779	*KRT16*	Keratin 16; keratin type 16-like
13	Q2VIQ3	*KIF4A*	Kinesin family member 4B; kinesin family member 4A
14	Q9BW19	*KIFC1*	Kinesin family member C1
15	P19105	*MYL12A*	Myosin, light chain 12A, regulatory, non-sarcomeric
16	Q9Y266	*NUDC*	Nuclear distribution gene C homolog (*A. nidulans*)
17	P62714	*PPP2CB*	Protein phosphatase 2 (formerly 2A), catalytic subunit, beta isoform
18	Q15019	*SEPT2*	Septin 2

19	Q76I76	*SSH2*	Slingshot homolog 2 (*Drosophila*)
20	O15020	*SPTBN2*	Spectrin, beta, non-erythrocytic 2
21	Q13425	*SNTB2*	Syntrophin, beta 2 (dystrophin-associated protein A1, 59 kDa, basic component 2)
22	O75347	*TBCA*	Tubulin folding cofactor A

Discussion

In this chapter, we successfully constructed an *in vitro* co-culture system of normal and *Scribble* knockout cells using HEK293T, a human-derived epithelial cell line, and analyzed the cellular changes that occur in the co-cultured cells caused by this gene transformation. *Scribble* is a well-known tumor suppressor gene that is known to be involved in several kinds of human cancers (8, 9). Therefore, it can be considered that this model system of co-culture represents the onset of cancer caused by the loss of *Scribble* expression, where few transformed cells are surrounded by a larger number of normal cells in an organism. Instead of considering a group of cancer cells as a population of cells with particular cancer gene transformations and identical characteristics to each other, present approach focuses on the heterogeneous nature of the cancer development process, in which normal cells and different types of transformed cells are mixed and interacting with each other.

By performing a thorough analysis of the proliferation rate of cells in fixed microscopic fields in co-culture systems, it was determined that when *Scribble* knockout cells (KO#18 strain) were co-cultured with wild-type cells, they proliferated at a higher rate than negative control GFP^+ cells (D#1 strain) (Fig. 4). Considering the fact that all conditions in the two co-culture systems using KO#18 or D#1 cells were identical except for the presence of the *Scribble* knockout, this result indicated that the transformation of the tumor suppressor gene *Scribble* functioned in a way that was beneficial for maintaining cell proliferation in co-culture with wild-type cells. In previous studies using *D. melanogaster* or the dog-derived epithelial cell line Madin-Darby Canine Kidney (MDCK) cell line, it has been shown that the loss of *Scribble*

leads to apoptosis and elimination of the transformed cells from the cell layer when co-cultured with normal cells (5, 10). However, the present study using human-derived cells showed contrary results, indicating that the influence of particular gene transformation may differ among different model systems using different species.

To investigate the molecular changes that occur in normal cells as a result of co-culture with *Scribble* knockout cells, whole protein profiles of the cells separated from the co-culture system were analyzed. Among the proteins that were specifically identified from wild-type cells in co-culture with *Scribble* knockout cells (139 proteins), it was discovered that cytoskeleton-related proteins (22 proteins), particularly microtubule motor activity-related proteins, were noticeably enriched. This result implied that when few cells with transformations in the tumor suppressor gene *Scribble* emerge among a population of normal cells, the surrounding normal cells respond to this change in the cell population with the reorganization of cytoskeletal structure and activation of cell mobility. This assumption is compatible with previous reports regarding cancer-related cell competition in MDCK cells, which have stated that cytoskeletal proteins, such as Filamin and EPLIN, are involved in the elimination of transformed cells in co-culture with normal cells (19, 20). The results from present research implied that molecular changes in cytoskeletal proteins occur in normal cells when co-cultured with *Scribble* knockout cells, but the beneficial influence of the *Scribble* knockout on proliferation of the transformed cells outcompetes this defense mechanism of the surrounding normal cells.

Summary

In very early stages of cancer development, few cells bearing transformation in cancer genes or tumor suppressor genes co-exist with a much larger number of surrounding normal cells. Recent studies using epithelial cells derived from *D. melanogaster* or dog have shown that intercellular interaction between normal and transformed cells occurs when mixed together, and the outcompeted type of cells undergo apoptosis or are eliminated from the cell layer. Elucidating the molecular mechanism underlying this interaction can be expected to lead to a novel approach toward cancer control. In this chapter, a co-culture system of normal and tumor suppressor gene *Scribble* knockout cells was constructed using a human-derived cell line HEK293T, and the cellular changes that occurred as a result of the co-culture were investigated. By thorough investigation of time-course change of the number of *Scribble* knockout cells when co-cultured with normal cells, it was found out that *Scribble* knockout is beneficial for the proliferation of cells in a situation where they have to compete with normal cells for survival and proliferation. Moreover, by performing proteome analysis on normal cells separated from the co-culture system with *Scribble* knockout cells or negative control GFP^+ cells, it was shown that a number of proteins that are involved in the cytoskeletal structure and motor activity of cells were specifically identified only from cells that were co-cultured with *Scribble* knockout cells. This result indicated that the normal cells correspond to the emergence of *Scribble* knockout cells by inducing changes in cytoskeletal structure and cell mobility.

References

1. **Sommers CL, Byers SW, Thompson EW, Torri JA, Gelmann EP.** 1994. Differentiation state and invasiveness of human breast cancer cell lines. Breast Cancer Res Treat **31:**325-335.

2. **Jogi A, Vaapil M, Johansson M, Pahlman S.** 2012. Cancer cell differentiation heterogeneity and aggressive behavior in solid tumors. Ups J Med Sci **117:**217-224.

3. **Moreno E, Basler K.** 2004. dMyc transforms cells into super-competitors. Cell **117:**117-129.

4. **Tamori Y, Bialucha CU, Tian AG, Kajita M, Huang YC, Norman M, Harrison N, Poulton J, Ivanovitch K, Disch L, Liu T, Deng WM, Fujita Y.** 2010. Involvement of Lgl and Mahjong/VprBP in cell competition. PLoS Biol **8:**e1000422.

5. **Norman M, Wisniewska KA, Lawrenson K, Garcia-Miranda P, Tada M, Kajita M, Mano H, Ishikawa S, Ikegawa M, Shimada T, Fujita Y.** 2012. Loss of Scribble causes cell competition in mammalian cells. J Cell Sci **125:**59-66.

6. **Bilder D, Perrimon N.** 2000. Localization of apical epithelial determinants by the basolateral PDZ protein Scribble. Nature **403:**676-680.

7. **Zhan L, Rosenberg A, Bergami KC, Yu M, Xuan Z, Jaffe AB, Allred C, Muthuswamy SK.** 2008. Deregulation of scribble promotes mammary tumorigenesis and reveals a role for cell polarity in carcinoma. Cell **135:**865-878.

8. **Navarro C, Nola S, Audebert S, Santoni MJ, Arsanto JP, Ginestier C, Marchetto S, Jacquemier J, Isnardon D, Le Bivic A, Birnbaum D, Borg JP.** 2005. Junctional recruitment of mammalian Scribble relies on E-cadherin engagement. Oncogene **24:**4330-4339.

9. **Gardiol D, Zacchi A, Petrera F, Stanta G, Banks L.** 2006. Human discs large and

scrib are localized at the same regions in colon mucosa and changes in their expression patterns are correlated with loss of tissue architecture during malignant progression. Int J Cancer **119:**1285-1290.

10. **Brumby AM, Richardson HE.** 2003. Scribble mutants cooperate with oncogenic Ras or Notch to cause neoplastic overgrowth in Drosophila. EMBO J **22:**5769-5779.

11. **Geiger T, Wehner A, Schaab C, Cox J, Mann M.** 2012. Comparative proteomic analysis of eleven common cell lines reveals ubiquitous but varying expression of most proteins. Mol Cell Proteomics **11:**M111 014050.

12. **Aburaya S, Esaka K, Morisaka H, Kuroda K, Ueda M.** 2015. Elucidation of the recognition mechanisms for hemicellulose and pectin in Clostridium cellulovorans using intracellular quantitative proteome analysis. AMB Express **5:**29.

13. **Morisaka H, Matsui K, Tatsukami Y, Kuroda K, Miyake H, Tamaru Y, Ueda M.** 2012. Profile of native cellulosomal proteins of Clostridium cellulovorans adapted to various carbon sources. AMB Express **2:**37.

14. **Motokawa M, Kobayashi H, Ishizuka N, Minakuchi H, Nakanishi K, Jinnai H, Hosoya K, Ikegami T, Tanaka N.** 2002. Monolithic silica columns with various skeleton sizes and through-pore sizes for capillary liquid chromatography. J Chromatogr A **961:**53-63.

15. **Huang da W, Sherman BT, Lempicki RA.** 2009. Systematic and integrative analysis of large gene lists using DAVID bioinformatics resources. Nat Protoc **4:**44-57.

16. **Huang da W, Sherman BT, Lempicki RA.** 2009. Bioinformatics enrichment tools: paths toward the comprehensive functional analysis of large gene lists. Nucleic Acids Res **37:**1-13.

17. **Jinek M, Chylinski K, Fonfara I, Hauer M, Doudna JA, Charpentier E.** 2012. A

programmable dual-RNA-guided DNA endonuclease in adaptive bacterial immunity. Science **337:**816-821.

18. **Mali P, Yang L, Esvelt KM, Aach J, Guell M, DiCarlo JE, Norville JE, Church GM.** 2013. RNA-guided human genome engineering via Cas9. Science **339:**823-826.

19. **Kajita M, Sugimura K, Ohoka A, Burden J, Suganuma H, Ikegawa M, Shimada T, Kitamura T, Shindoh M, Ishikawa S, Yamamoto S, Saitoh S, Yako Y, Takahashi R, Okajima T, Kikuta J, Maijima Y, Ishii M, Tada M, Fujita Y.** 2014. Filamin acts as a key regulator in epithelial defence against transformed cells. Nat Commun **5:**4428.

20. **Ohoka A, Kajita M, Ikenouchi J, Yako Y, Kitamoto S, Kon S, Ikegawa M, Shimada T, Ishikawa S, Fujita Y.** 2015. EPLIN is a crucial regulator for extrusion of RasV12-transformed cells. J Cell Sci **128:**781-789.

Conclusions

The present studies have been carried out to analyze cellular changes that occur during cell differentiation processes at the single cell level.

In chapter I, I analyzed the neuronal differentiation process of PC12 rat pheochromocytoma cells at the single cell level, by using the automated direct microinjection method. Accurate regulation of a chemical agent introduced into individual target cells was made possible, and the inhibitive effect on each single cell was analyzed quantitatively. By using this method, PC12 differentiation was successfully inhibited even when using lower amount of U0126 compared with existing methods, without being affected by the surrounding environment of target cells. Furthermore, it was shown that the neuronal differentiation of PC12 cells was not a one-way process that only leads to the growth of neurites, but a dynamic bidirectional process involving both growing and shrinking of neurites, which is largely variable across individual cells. This chapter highlights the effectiveness of direct microinjection method for rigorous control of the amount of differentiation-regulating factors introduced into individual target cells and analysis of the outcomes at the single cell level.

In chapter II, I elucidated the cellular changes induced by the co-culture of normal HEK293T cells and cells with the loss of tumor suppressor gene, *Scribble*. By analyzing the time-course changes in cell numbers when *Scribble* knockout cells or negative control GFP^+ cells were respectively co-cultured with wild-type cells, it was shown that *Scribble* knockout functions in a way that is beneficial for proliferation of the transformed cells when mixed together with normal cells. This result also indicated that the influence of cancer-related transformation on cells can be variable depending on the species. Moreover, as a result of proteome analysis on wild-type cells separated from co-culture with *Scribble* knockout cells, a total of 843 proteins were identified. Among the 139 proteins that were specifically identified from cells co-cultured with *Scribble* knockout cells but not from cells co-cultured with the negative control cells, 22 proteins were annotated to be involved in cytoskeleton and microtubule motor activity. It was implied that molecular changes in cytoskeletal proteins occur in normal cells when co-cultured with *Scribble* knockout cells, but the beneficial influence of *Scribble* knockout on proliferation of the transformed cells outcompetes this defense mechanism of surrounding normal cells.

Acknowledgements

This thesis is submitted by the author to Kyoto University for the Doctor degree of Agriculture. The studies presented here have been carried out under the direction of Professor Mitsuyoshi Ueda in the Laboratory of Biomacromolecular Chemistry, Division of Applied Life Sciences, Graduate School of Agriculture, Kyoto University, during 2009-2016.

I would like to express my greatest appreciation to Professor Mitsuyoshi Ueda for his continuous support by insightful comments, meaningful discussions, and warm patience, throughout the course of this study.

I deeply thank Associate Professor Kouichi Kuroda for his guidance and advices throughout my study. I would also like to express my sincere gratitude to the late Dr. Hironobu Morisaka, the Assistant Professor who always provided critical comments and feedbacks about this research, and thoughtfully supported me with warm heart. I would also like to thank the Assistant Professor Wataru Aoki for valuable advices and discussions regarding this research. I express my appreciation to the secretary Fukuko Suzuki for her kind support of my laboratory life. I would like to thank each and one of my colleagues in the laboratory for valuable discussion concerning this research, constant encouragements and supports.

I express my sincerest gratitude to Samsung Scholarship, Kashiyama Scholarship Foundation, Ichikawa International Scholarship Foundation, and Iwatani Foundation for financial supports.

Lastly, I would like to sincerely thank my family for their warm love, deep understanding and continuous support throughout this research.

JI-HYE CHUNG

Laboratory of Biomacromolecular Chemistry
Division of Applied Life Sciences
Graduate School of Agriculture
Kyoto University

Publications

Chapter I

Chung J, Miura N, Ito A, Sawada M, Nishikawa S, Kuroda K, Ueda M. 2014. Single-cell heterogeneity in suppression of PC12 differentiation by direct microinjection of a differentiation inhibitor, U0126. Cell Biol Int **38:** 1215-1220

Chapter II

Chung J, Aburaya S, Miura N, Aoki W, Ueda M. Cellular changes induced by co-culture of normal HEK293T cells with *Scribble* knockout cells. In preparation.